Acta Oceanol. Sin., 2024, Vol. 43, No. 4, P. 119–135
https://doi.org/10.1007/s13131-024-2333-8
http://www.aosocean.com
E-mail: ocean2@hyxb.org.cn

Formation environment and hydrocarbon potential of the Paleogene Enping Formation coal measures in the Zhu Ⅰ Depression of northern South China Sea

Yuting Yin[1], Lei Lan[2], Dongdong Wang[1, 3*], Ying Chen[2], Yan Liu[1], Youchuan Li[2], Zengxue Li[1], Jiamin Liu[1]

[1] College of Earth Science and Engineering, Shandong University of Science and Technology, Qingdao, Shandong 266590, China

[2] China National Offshore Oil Corporation Research Institute Co., Ltd., Beijing 100028, China

[3] School of Geography, Earth and Environmental Sciences, University of Birmingham, Birmingham, B15 2TT, UK

Received 30 May 2023; accepted 13 September 2023

© Chinese Society for Oceanography and Springer-Verlag GmbH Germany, part of Springer Nature 2024

Abstract

The coal-measure source rock in the Chinese sea area plays a significant role as a hydrocarbon source rock, with its genetic environment, development and distribution, and hydrocarbon generation potential serving as essential factors for the exploration of coal-type oil and gas fields. This study focuses on the coal-measure source rock of the Paleogene Enping Formation in the Zhu Ⅰ Depression, located in the northern South China Sea. The main geological insights obtained are as follows. The coal measures of the Enping Formation are developed in a warm and wet tropical-subtropical climate. The development environment of the coal-measure source rock in the Enping Formation includes the braided river delta upper plain peat swamp, characterized by dry forest swamp coal facies with relatively thick coal seams and a small number of layers. The braided river delta lower plain swamp-interdistributary bay of braided river delta front represents a forest edge-wetland herbaceous swamp coal facies with numerous layers of thin coal seams and poor stability. The shore swamp corresponds to an open water swamp coal facies with multiple layers of thin coal seams and poor stability. The organic matter abundance in the braided river delta upper plain is the highest, followed by the braided river delta lower plain-braided river delta front, and the shore-shallow lake. The organic matter type is predominantly type Ⅱ_1. Thermal evolution analysis suggests that the organic matter has progressed into a substantial oil generation stage. The hydrocarbon generation potential of the coal-measure source rock in the Enping Formation is the highest in the braided river delta upper plain, followed by the braided river delta lower plain-braided river delta front and the shore-shallow lake. Overall, this study proposes three organic facies in the coal-measure source rock of the Enping Formation: upper-plain swamp-dry forest swamp facies, lower plain-interdistributary bay-forest-herbaceous swamp facies, and lake swamp-herbaceous swamp facies.

Key words: coal-measure source rock, Paleogene, genetic environment, hydrocarbon generation characteristic, Zhu Ⅰ Depression

Citation: Yin Yuting, Lan Lei, Wang Dongdong, Chen Ying, Liu Yan, Li Youchuan, Li Zengxue, Liu Jiamin. 2024. Formation environment and hydrocarbon potential of the Paleogene Enping Formation coal measures in the Zhu Ⅰ Depression of northern South China Sea. Acta Oceanologica Sinica, 43(4): 119–135, doi: 10.1007/s13131-024-2333-8

1 Introduction

With the progressive expansion of oil and gas exploration activities, the sea has become the key area for such endeavors. The South China Sea (SCS) is recognized as a world-class oil and gas region, having witnessed the discovery of numerous large-scale oil and gas fields (Deng and Chen, 1989; Zhang et al., 2007, 2016a, 2017a, 2017b). Among the oil and gas resources in China' sea area, coal-type oil and gas reserves dominate, with the coal-measure source rock serving as a pivotal hydrocarbon source rock (Li et al., 2014; Zhang et al., 2022, 2023). The coal-measure source rock from the Oligocene Yacheng Formation and Enping Formation predominantly occur in the Qiongdongnan Basin and the Baiyun Sag of the Pearl (Zhujiang) River Mouth Basin in the northern SCS (Zhang et al., 2007, 2019; Fu et al, 2010; Wang et al., 2011; Li et al., 2011; Huang et al., 2014; Pang et al., 2014). In the central and southern basins of the SCS, the coal-measure source rock development spans the Oligocene-Pliocene period, primarily occurring during the Miocene and Pliocene epochs (Yao et al, 2008; Yang et al., 2010; Xie et al., 2011). The coal-measure source rock in the northern SCS basin mainly derives organic matter from terrigenous higher plants, with the river delta system exerting a crucial influence on the growth of these plants and the organic matter enrichment. Consequently, the coal-measure source rock formed in such environments exhibits high hydro-

Foundation item: The Scientific research project under contract under contract No. CCL2021RCPS172KQN; Formation mechanism and distribution prediction of Cenozoic marine source rocks in Qiongdongnan and Pearl River Mouth Basin under contract No. 2021-KT-YXKY-01; the resource potential, accumulation mechanism and breakthrough direction of potential oil-rich sags in offshore basins of China under contract No. 2021-KT-YXKY-03; the Open Foundation of Hebei Provincial Key Laboratory of Resource Survey and Research; the National Natural Science Foundation of China (NSFC) under contract Nos 42072188, 42272205.
*Corresponding author, E-mail: wdd02_1@163.com

carbon generation potential (Li et al., 2011, 2014; Deng et al., 2019; Gao et al., 2022). The Xihu Depression is one of the most hydrocarbon-rich Neogene basins in the East China Sea Shelf Basin. It has high organic matter abundance. The organic matter type is predominantly type Ⅱ and type Ⅲ kerogens. The organic matter is generally in a mature stage, with only a small portion in the low maturity and high maturity stages. The organic matter is derived from terrigenous higher plants and possesses a high hydrocarbon generation potential（Shen, 2018; Kang et al., 2020; Li et al., 2022）. Different coal facies and sedimentary organic facies within the coal-measure source rock exhibit significant variations in hydrocarbon generation characteristics (Yang et al., 2000; Xie and Zhao, 2015). Presently, studies on the sedimentary environment and the hydrocarbon generation potential of the coal-measure source rock in China's sea areas are scarce and predominantly focused on in the northern SCS Basin and shallow-water environments of the East China Sea Basin (Li et al., 2010; Zhang et al., 2010, 2016b, 2019; Shen et al., 2016; Shen, 2018; Wang et al., 2020). Consequently, the understanding of the genetic conditions, control factors, hydrocarbon generation characteristics, and the hydrocarbon generation potential of the the coal-measure source rock in China's sea areas remains limited, hindering the exploration and development of coal-type oil and gas resources in China's sea area.

This paper focuses on the coal-measure source rock of the Paleogene Enping Formation in the Zhu Ⅰ Depression within the Pearl (Zhujiang) River Mouth Basin. It analyzes the genetic conditions, controlling factors, hydrocarbon generation characteristics, and the hydrocarbon generation potential of the coal-measure source rock, while proposing a typical sedimentary organic facies model. The study aims to provide valuable theoretical support for the exploration of coal-type oil and gas source rocks in China's sea areas.

2 Regional geological background

2.1 *Structural location and evolution*

The Pearl (Zhujiang) River Mouth Basin is located on the northern slope of the SCS and is a Cenozoic basin formed on the Caledonian, Hercynian, and Yanshanian fold basements, covering an area of about 175 000 km^2. The basin is mainly controlled by the NE and NWW fault zones and is generally distributed in a NE–SW direction. The structural pattern exhibits characteristics of "three uplifts and two depressions" and "east-west block, north-south zoning" (Wu, 2013). The Zhu Ⅰ Depression is situated in the middle-east of the Northern Depression Belt of the Pearl (Zhujiang) River Mouth Basin. Its northern part is the Northern Uplift Belt, the western part is the Zhu III Depression, and the southern part comprises the Dongsha Uplift and the Panyu Low Uplift. The tectonic framework of the Zhu Ⅰ Depression is primarily controlled by the NW low uplift and NE fault system (Wu, 2013), consisting of Enping Sag, Xijiang Sag, Huizhou Sag, Lufeng Sag, Hanjiang Sag, Huilu Low Uplift, and several secondary uplifts (Zhu et al., 2014; Liu et al., 2017; Ding et al., 2022) (Fig. 1a).

The Cenozoic tectonic evolution of the Pearl (Zhujiang) River Mouth Basin can be divided into three stages. (1) Fault-Depression Stage: The pre-Cenozoic basement of the northern continental margin of the SCS underwent rifting, resulting in a rift zone and a typical angular unconformity in the northern Pearl (Zhujiang) River Mouth Basin (Fig. 2a). (2) Depression Stage: The basin experienced significant uplift, stratigraphic erosion, faults, and magmatic activities, leading to regional unconformities (Fig. 2b). (3) Block Break Lifting Stage: In the post-rift stage, the basin witnessed block fault lifting, compression deformation, uplift erosion, and volcanic magmatic activity on a small range (Fig. 2c). Since the Cenozoic, the Zhu Ⅰ Depression has undergone various tectonic movements, such as the Shenhu Movement, the Zhuqiong Movement, the South China Sea Movement, and the Dongsha Movement. Among these, the South China Sea Movement serves as the transitional symbol between the Chasmic Stage and the Depression Stage. The tectonic movements corresponding to the Chasmic Stage include the Shenhu Movement, the Zhuqiong I Movement, and the Zhuqiong Ⅱ Movement. The Depression Stage corresponds to the South China Sea Movement, while the Block Break Lifting Stage corresponds to the Dongsha Movement (Shu et al., 2014). The deposition of the Enping Formation mainly occurred during the Zhuqiong Ⅱ Move-

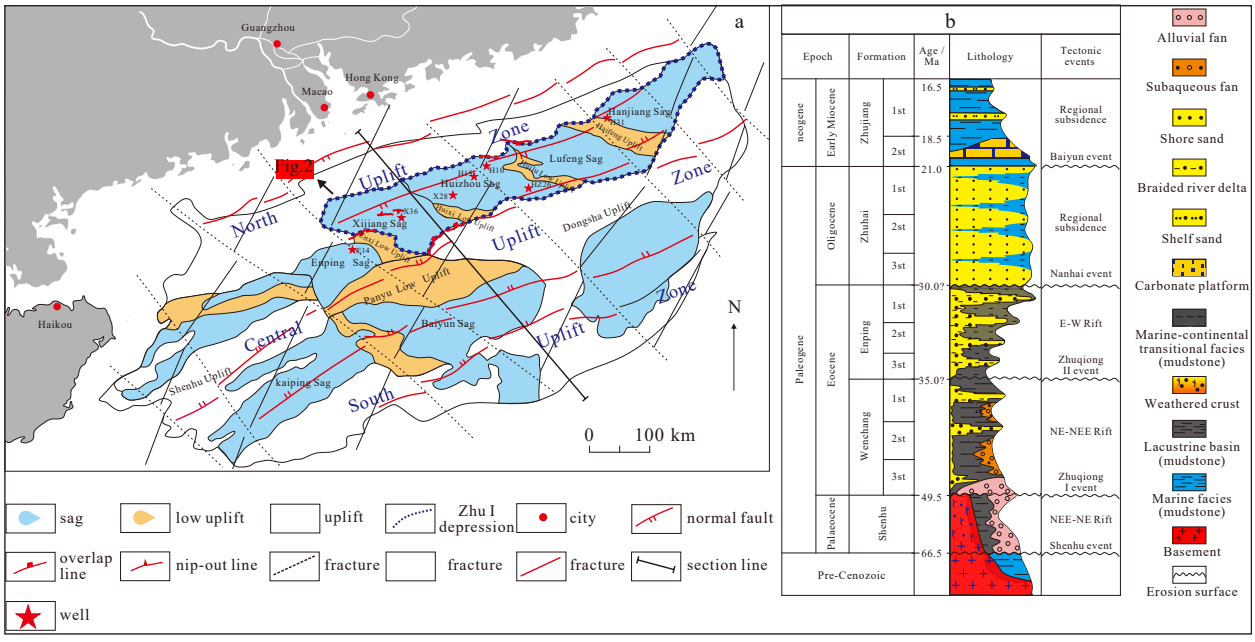

Fig. 1. Geographical location and structural geological map of the Pearl (Zhujiang) River Mouth Basin (modified from Jiang et al., 2009; Zhang et al., 2020; Wei et al., 2020).

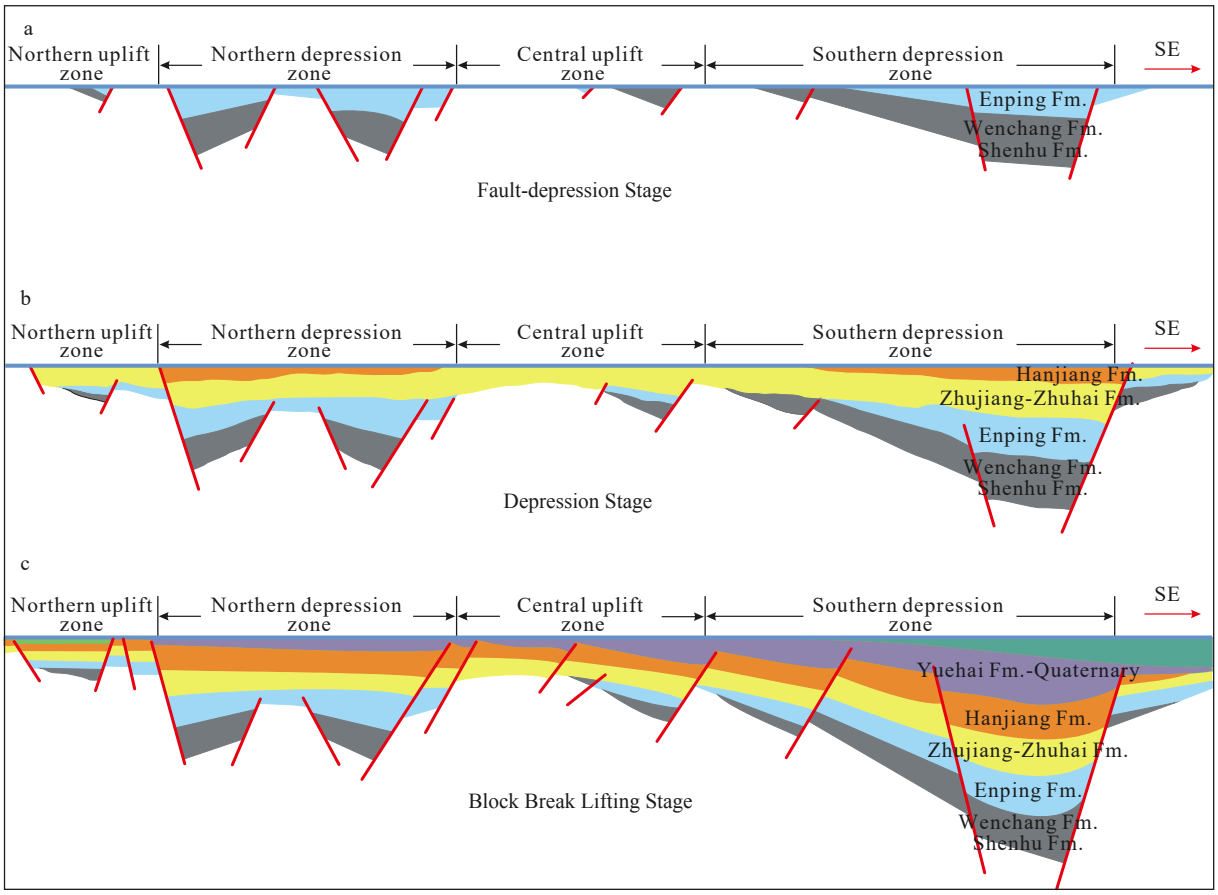

Fig. 2. Evolution stage diagram of the Pearl (Zhujiang) River Mouth Basin (modified from Wu, 2013).

ment. During this period, strong and prolonged tectonic movements led to significant uplift and erosion of the basin, resulting in the formation of a large-scale EW-trending fault system in the Zhu Ⅰ Depression. In this tectonic stage, the lake basin area is larger than during the Zhuqiong Ⅰ Movement, but the lake water is shallower. The Southern Depression Belt and the Northern Depression Belt began connecting in the late Enping Formation.

2.2 *The development of strata and coal measures*

In the Zhu Ⅰ Depression, the Paleogene and Neogene periods mainly witnessed the development of the Shenhu Formation, Wenchang Formation, Enping Formation, Zhuhai Formation, and Zhujiang Formation, with well-developed strata.

The Shenhu Formation was formed during the early stage of the rifting of the Zhuqiong Movement, ranging from the Paleocene to the early Eocene, and is in unconformity contact with the overlying strata (Fig. 1b). It primarily consists of interbedded sandstone and mudstone with a small thickness and visible glutenite and volcanic rocks.

The Wenchang Formation was formed during the rifting episode of the Eocene Zhuqiong Ⅰ Movement and has a thickness of about 1 000 m. It mainly comprises mudstone, thin sandstone, and siltstone, with occasional coal seams (Fig. 1b).

The Enping Formation was formed during the Zhuqiong Ⅱ Movement in the late Eocene to early Oligocene rifting period, with a thickness of about 800 m. It mainly consists of thick sandstone with thin mudstone, locally exhibiting coal seams or coal lines. The coal measures have a large thickness and a significant number of coal layers, but individual layers are thin, typically around 1 m. They exhibit poor stability with scattered vertical distribution and wide plane distribution. Additionally, a significant amount of charcoal mudstone is present. The Enping Formation is in unconformity contact with the overlying and underlying strata (Fig. 1b) (Li, 2015).

The Zhuhai Formation was formed during the late Oligocene fault-depression transition period and has a thickness of about 400 m. It primarily consists of light gray, medium-thick medium sandstone, with some medium-thin mudstone and sporadic thin coal seams (Fig. 1b).

The Zhujiang Formation was formed during the Depression Stage of the early Miocene basin and has a thickness of about 700 m. It mainly comprises gray calcareous mudstone or limestone, occasionally interbedded with thin siltstone (Fig. 1b).

3 Genetic conditions of the coal-measure source rock in enping formation

3.1 *Relationship between ancient plant and paleoclimate characteristics and Coal seam development*

Ancient plants are the material basis for coal formation and the prerequisite for the development of coal seams. Moreover, different types of coal-forming plants affect the type and content of coal macerals (Dai et al., 2020). In the Enping Formation of the Zhu Ⅰ Depression, the most common types of sporopollen are from angiosperms (*Tricolpopollenites, Triporopollenites*), and ferns (*Polypodiaceaesporites, Polypodiisporites*), while gymnosperm pollen (*Pinuspollenites*) is less common. The content of phytoplankton (*Homotryblium, Pediastrum*) is very low (Fig. 3).

The typical sporopollen types of the Enping Formation in the Zhu Ⅰ Depression are analyzed using ordered cluster analysis,

resulting in the division of four sporopollen zones from bottom to top (Fig. 4) (The original data come from CNOOC Research Institute, 2007).

Sporopollen zone Ⅰ: The main sporopollen assemblage consists of *Pinuspollenites, Taxodiaceaepollenites, Tricolpopollenites, Tricolporopollenites,* and other perforated classes, Polypodiaceaesporites, Osmundacidites. The dominant plant type is *Tricolpopollenites* and *Tricolporopollenites* of *Fagaceae*, followed by *Polypodiaceaesporites* of *Fern.* The content of *Alnipollenites*, *Liquidambarpollenites,* and *Ulmipollenites* from deciduous trees is relatively low as is the content of *Pinuspollenites* and *Taxodiaceaepollenites* from evergreen trees.

Sporopollen zone Ⅱ: The main sporopollen assemblage consists of *Pinuspollenites, Taxodiaceaepollenites, Tricolpopollenites, Tricolporopollenites,* and other perforated classes, Polypodiaceaesporites. The dominant plant type is *Tricolpopollenites* and *Tricolporopollenites* of *Fagaceae*, with a higher content compared to sporopollen zone Ⅰ. The content of *Polypodiaceaesporites* in *Ferns* is lower than in sporopollen zone Ⅰ. The content of *Pinuspollenites* and *Taxodiaceaepollenites* in evergreen trees is lower than the content in sporopollen zone Ⅰ. Also, the content of *Alnipollenites*, *Liquidambarpollenites,* and *Ulmipollenites* from deciduous trees is relatively low, lower than in sporopollen zone Ⅰ.

Sporopollen zone Ⅲ: The main sporopollen assemblage consists of *Pinuspollenites, Taxodiaceaepollenites, Tricolpopollenites, Tricolporopollenites,* and other perforated classes, Polypodiaceaesporites. The dominant plant type is still *Tricolpopollenites* and *Tricolporopollenites* of *Fagaceae*, with a lower content than in sporopollen zone Ⅱ. The content of *Polypodiaceaesporites* in *Ferns* is higher than in sporopollen zone Ⅱ. Also, the content of *Pinuspollenites* and *Taxodiaceaepollenites* in evergreen trees is lower than the content in sporopollen zone Ⅱ, while the content of *Alnipollenites*, *Liquidambarpollenites,* and *Ulmipollenites* in deciduous trees is relatively low, lower than in sporopollen zone Ⅱ.

Sporopollen zone Ⅳ: The main sporopollen assemblage consists of *Pinuspollenites, Tricolpopollenites, Tricolporopollenites*, and *other perforated classes, Polypodiaceaesporites.* The dominant plant type is *Tricolpopollenites* and *Tricolporopollenites* of *Fagaceae*, with a lower content than in sporopollen zone Ⅲ. The second is the *Polypodiaceaesporites* of *Fern*, with a much lower content than in sporopollen zone Ⅲ, followed by the evergreen trees of *Pinuspollenites* and *Taxodiaceaepollenites*, with their content showing no significant change compared to sporopollen zone Ⅲ. The content of *Alnipollenites*, *Liquidambarpollenites,* and *Ulmipollenites* in deciduous trees is relatively low, but significantly higher than in sporopollen zone Ⅲ.

The overall trend in plant type changes during the sedimentary period of the Enping Formation is that *Fagaceae* are dominant, with an increase in content in sporopollen zone Ⅱ, but a decrease from early to late stages. *Ferns* shows an increasing trend in content in sporopollen zone Ⅲ, but an overall downward trend. Evergreen trees follow a decreasing trend content from early to late, but show an in sporopollen zone Ⅱ. The content of deciduous trees is relatively low, decreasing from early to late but increasing significantly in sporopollen zone Ⅳ.

In summary, the typical sporopollen assemblage in the Enping Formation coal measures is the *Dicolpopllos kockolii-Gothanipollis bassensis* assemblage, with little to no *Fern* presence. This sporopollen assemblage reflects an ancient vegetation type of evergreen broad-leaved forests during the sedimentary period of the Enping Formation. Greenery and broad-leaved species comprise the main components (Guo, 2015). *Pinuspollenites*, *Tsugaepollenites,* and other plants grow in the mountainous environments surrounding the basin. *Fagaceae* plants thrive on slopes, hills, and similar environments, while some *Palmae* grow on plains. Swamp wetlands may exist in certain areas of the basin, supporting the growth of wetland plants. Various *Fern* species grow in wet areas of mountain slopes or plain forests, freshwater phytoplankton thrives in deep water environments (Fig. 3) (Yao, 2006).

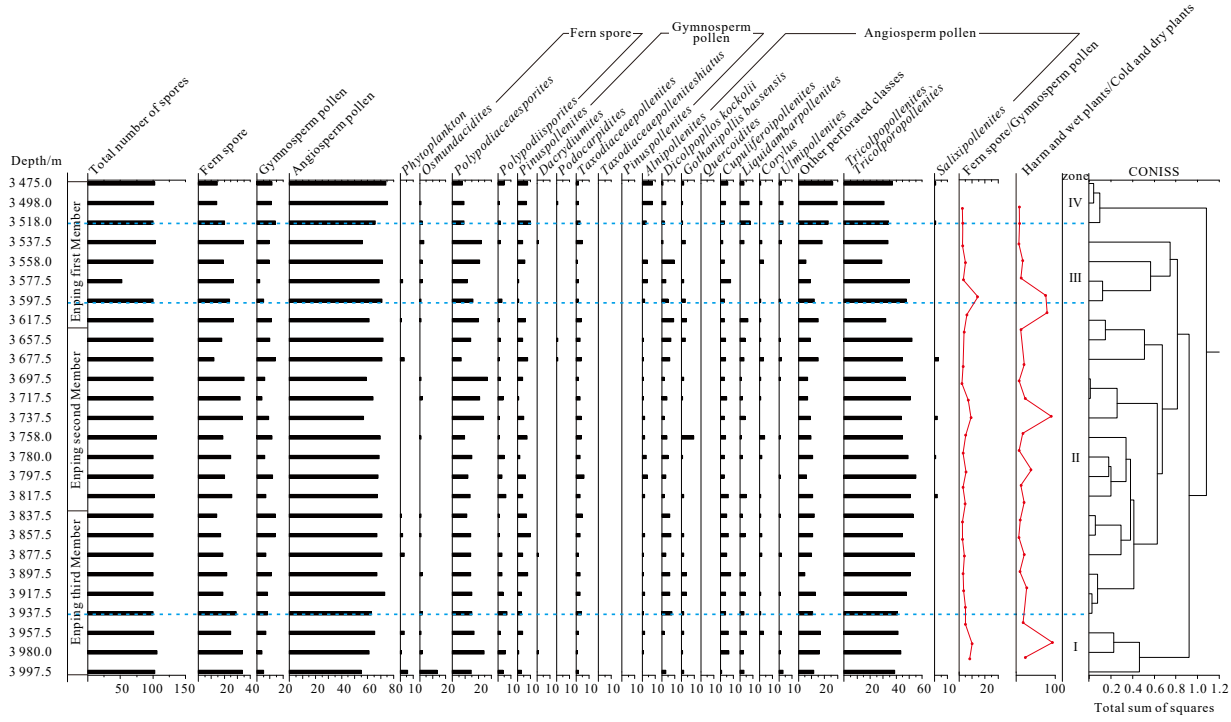

Fig. 3. Pollen cluster analysis of X28 well in Zhu Ⅰ Depression, the Pearl (Zhujiang) River Mouth Basin The original data come from CNOOC Research Institute, 2007.

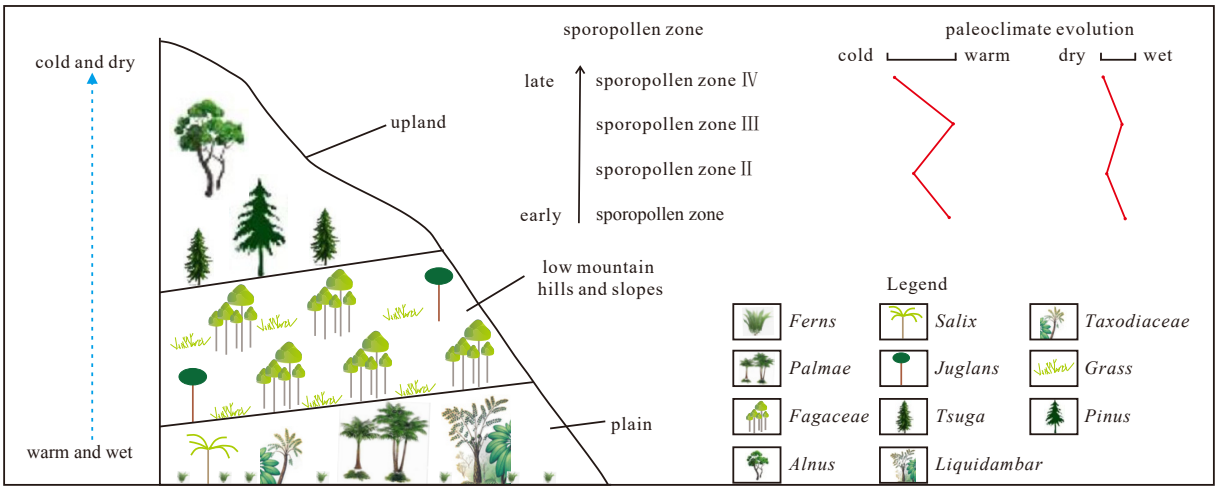

Fig. 4. Ancient plant restoration map of Paleogene Enping Formation in Zhu Ⅰ Depression.

The paleoclimate is one of the important controlling factors for the development of coal-forming plants and the occurrence of coal formation, which controls regional and temporal coal formation from a macro perspective (Dai et al., 2020). Sporopollen is the most direct and powerful evidence of paleoclimate.

According to the results of ordered cluster analysis of sporopollen data from the Enping Formation, the paleoclimate characteristics reflected by the four sporopollen zones of the Enping Formation are as follows (Fig. 4) (The original data come from CNOOC Research Institute, 2007).

Sporopollen zone Ⅰ: The dominant sporopollen assemblages representing warm and wet conditions are *Tricolpopollenites, Tricolporopollenites,* and *Polypodiaceaesporites*, with respective contents of 41.27 % and 18.63%. The second-highest content is in the *Perforated* class, at 14.83%. The sporopollen content of *Pinuspollenites* and *Taxodiaceaepollenites*, representing dry and cold conditions, is low, with contents of 2.60% and 1.60%, respectively. The ratio of *Fern* sporopollen content to gymnosperm sporopollen content is 6.94, indicating a warm and wet climate during this period. The content of Phytoplankton is 3.23%.

Sporopollen zone Ⅱ: There is no significant change in the total number of spores in this zone compared to zone Ⅰ. The content of Phytoplankton has decreased significantly, to 0.63%. Although the content of sporopollen *Pinuspollenites* and *Taxodiaceaepollenites,* representing dry and cold conditions, is slightly higher than in the early stage, with contents of 5.16% and 3.48%, respectively, the content of sporopollen in *Tricolpopollenites, Tricolporopollenites*, representing warm and wet conditions, has also increased compared to the previous period, with a content of 47.68%. The content of *Polypodiaceaesporites* has slightly reduced to 15.39%. The ratio of *Fern* sporopollen content to gymnosperm sporopollen content is 2.93, lower than in zone Ⅰ, indicating a warm and wet climate during this period, but with slightly lower humidity.

Sporopollen zone Ⅲ: The total number of spores in this zone is significantly lower than in zone Ⅱ. The content of *Pinuspollenites* and *Taxodiaceaepollenites*, representing dry and cold conditions, has decreased significantly compared to the previous period, with contents of 2.90% and 2.43%, respectively. The content of *Tricolpopollenites and Tricolporopollenites,* representing warm and wet conditions, is lower than in the early stage, but the content of *Polypodiaceaesporites* is higher than in the early stage, with contents of 40.13% and 17.65%, respectively. The ratio of *Fern* sporopollen content to gymnosperm content is 5.98, which is higher than in zone Ⅱ. The climate is becoming warmer and wetter during this period.

Sporopollen zone Ⅳ: The total number of spores in this zone is higher than in zone Ⅲ. The content of *Pinuspollenites* and *Taxodiaceaepollenites*, representing dry and cold conditions, has increased significantly compared to the previous period, with contents of 8.23% and 2.30%, respectively. The contents of *Tricolpopollenites*, *Tricolporopollenites,* and *Polypodiaceaesporites,* representing warm and wet conditions, are lower than in the early stage, with contents of 33.87% and 8.57%. The ratio of *Fern* sporopollen content to gymnosperm sporopollen content is 1.32, lower than in zone Ⅲ. The climate changes from warm and wet to dry and cold, with phytoplankton disappearing.

The general trend of sporopollen changes in the sedimentary period of the Enping Formation is as follows: The content of *Pinuspollenites,* representing dry and cold conditions, shows a slight downward trend in zone Ⅲ, but overall, it shows an upward trend, with significantly increased numbers in the later period compared to the previous period. The contents of *Tricolpopollenites*, *Tricolporopollenites,* and *Polypodiaceaesporites*, representing warm and wet conditions, increase in zone Ⅱ, but the overall trend is decreasing, with significantly lower numbers in the later stage compared to the early stage. This trend indicates that the paleoclimate gradually changes in a dry and cold direction. However, the overall climate in the study area does not fluctuate greatly and is mainly tropical-subtropical.

Additionally, some microelements can also indicate the paleoclimate. The enrichment of the Sr element is often related to a hot and dry climate (Wang and Zhang, 1996), and the Cu element in lake water mainly comes from atmospheric input and is less affected by external input (Lerman, 1989). The value of Sr/Cu is often used to reveal paleoclimate information, where Sr/Cu < 5.0 indicates a warm and wet climate and Sr/Cu > 5.0 indicates a hot and dry climate (Liu and Zhou, 2007). The Sr/Cu value of the Enping Formation in the Zhu Ⅰ Depression is less than 5.0 overall (Table 1), which also reflects the warm and wet climate during this period. In general, the sedimentary period of the Paleogene Enping Formation in the Zhu Ⅰ Depression belongs to a tropical-subtropical climate.

3.2 *Sedimentary environmental characteristics*

3.2.1 *Sedimentary environment characteristics of enping coal*

Tectonic activity has an impact on the sedimentary environment, which is the main factor influencing the formation of coal

Table 1. The trace element data table of the Paleogene Enping Formation in the Zhu Ⅰ Depression

Well	Sr/Ba	Sr/Cu	V/ (V+Ni)
X28	(0.12–0.34)/0.26 (7)	(0.33–1.56)/0.95 (7)	(0.79–0.83)/0.82 (7)
H15	(0.12–0.27)/0.17 (6)	(0.55–1.40)/0.95 (6)	(0.78–0.81)/0.80 (6)
X36	(0.25–0.41)/0.33 (4)	(1.54–3.81)/2.33 (4)	(0.80–0.84)/0.82 (4)

Note: (0.12–0.34)/0.26 (7) representation (min-max)/AVG (the No. of samples).

and peat swamps. In the Enping Formation of the Zhu Ⅰ Depression, various coal-forming environments can be identified, including braided river deltas, shore-shallow lakes, and fan deltas. Among them, the braided river delta plain and shore swamp are the most favorable for coal formation. During the sedimentary period of the Enping Formation in the Zhu Ⅰ Depression, the terrain was relatively flat, and the braided river delta extended over a large area, mainly consisting of shallow braided river deltas. The shallow braided river delta plain environment can be further subdivided into the upper and lower plains-front.

(1) Braided river delta upper plain: The peat swamp in this area has a wide distribution, and the sedimentary environment is relatively stable, promoting the formation of slightly thicker coal seams (Li et al., 2010). Currently, drilling data shows that the thickness of coal seams formed in this facies belt ranges from 0.40–1.50 m, with an average of 0.88 m (Table 2). The average thickness of coal seams is relatively large. The shallow water and nutrient-rich conditions support the growth and accumulation of plants, making this an important coal-forming environment during this period (Han and Wei, 2001) (Fig. 5a).

(2) Braided river delta lower plain-braided river delta front: In the interdistributary bay, the water is shallow and the hydrodynamics are weak, allowing for the localized development of peat swamps. However, this area is significantly influenced by lake water, leading to an unstable peat swamp environment and a large number of coal layers with small thickness and poor stability (Fig. 5b). Drilling data indicates that the coal seams formed in this facies belt range from 0.20-3.25 m in thickness, with an average of 0.79 m. The average thickness of coals seam is relatively small (Table 2).

(3) Shore-shallow lake: The shallow lake swamp with a small water depth is another important coal-forming environment during this period. Due to the frequent rise and fall of the lake level and the continuous development and destruction of shallow lake swamps, coal seams with multiple layers, thin thickness, and wide distribution are extensively developed (Fig. 5c). Drilling data reveals that the thickness of coal seams formed in this facies belt ranges from 0.30-2.25 m, with an average of 0.83 m. The average thickness of coal seams is medium (Table 2).

3.2.2 *Macerals and coal facies types of Enping Formation*

Macerals are organic components of coal that can be identified under a microscope. They are the degradation or residual products of various tissues and organs in plants. (Suárez-Ruiz and Crelling, 2008). In the Enping Formation coal of the Zhu Ⅰ Depression (10 samples), the vitrinite content ranges from 30.30%–98.10%, with an average of 80.30%. The liptinite content ranges from 1.30%-20.90%, with an average of 11.10%. The inertinite content ranges from 0–1.40%, with an average of 0.41% (Figs 6a and 7). In charcoal mudstone (15 samples), the vitrinite content ranges from 3.60%–29.10%, with an average of 16.10%, while the content of liptinite ranges from 2.10%–10.10%, with an average of fied under a microscope. They are the degradation or residual products of various tissues and organs in plants. (Suárez-Ruiz and Crelling, 2008). In the Enping Formation coal of the Zhu Ⅰ Depression (10 samples), the vitrinite content ranges

Table 2. Coal seam thickness table of different sedimentary facies of Paleogene Enping Formation in Zhu Ⅰ depression

Sedimentary facies	Braided river delta upper plain	Braided river delta lower plain-braided river delta front	Shore-shallow lake
Coal seam thickness/m	(0.40–1.50)/0.88 (22)	(0.20–3.25)/0.79 (391)	(0.30–2.25)/0.83 (97)

Note: (0.4–1.5)/0.88 (22) is (min-max)/AVG (the No. of samples).

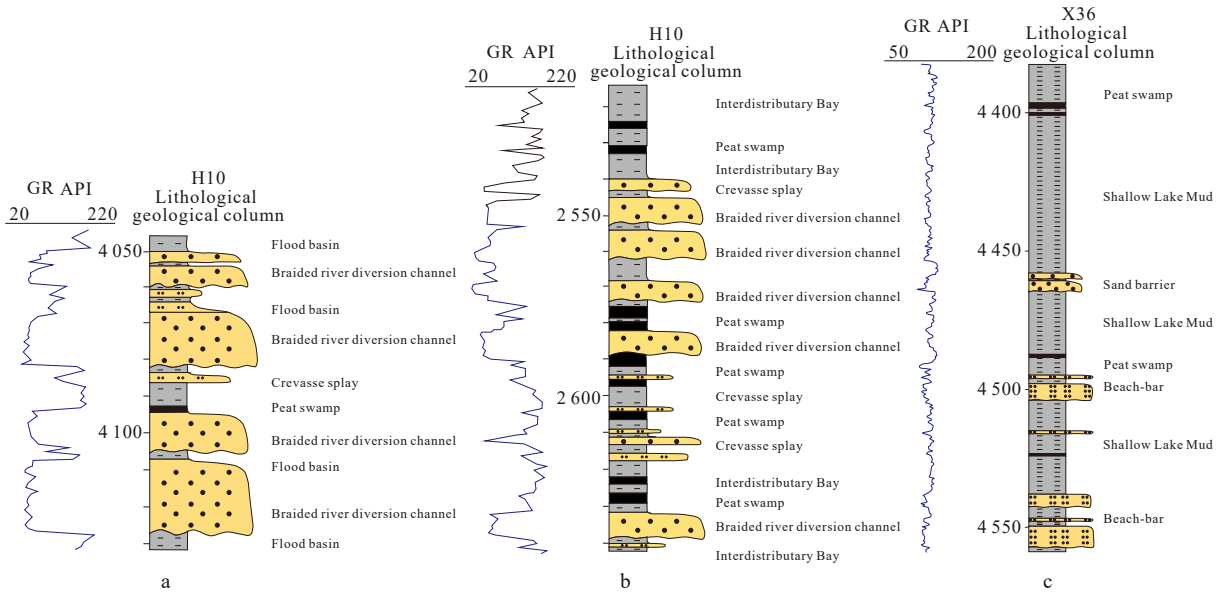

Fig. 5. Typical coal-forming sedimentary environment types of Enping Formation in Zhu Ⅰ Depression, the Pearl (Zhujiang) River Mouth Basin. a. Braided river delta upper plain; b. Braided river delta lower plain-braided river delta front; c. Shore-shallow lake.

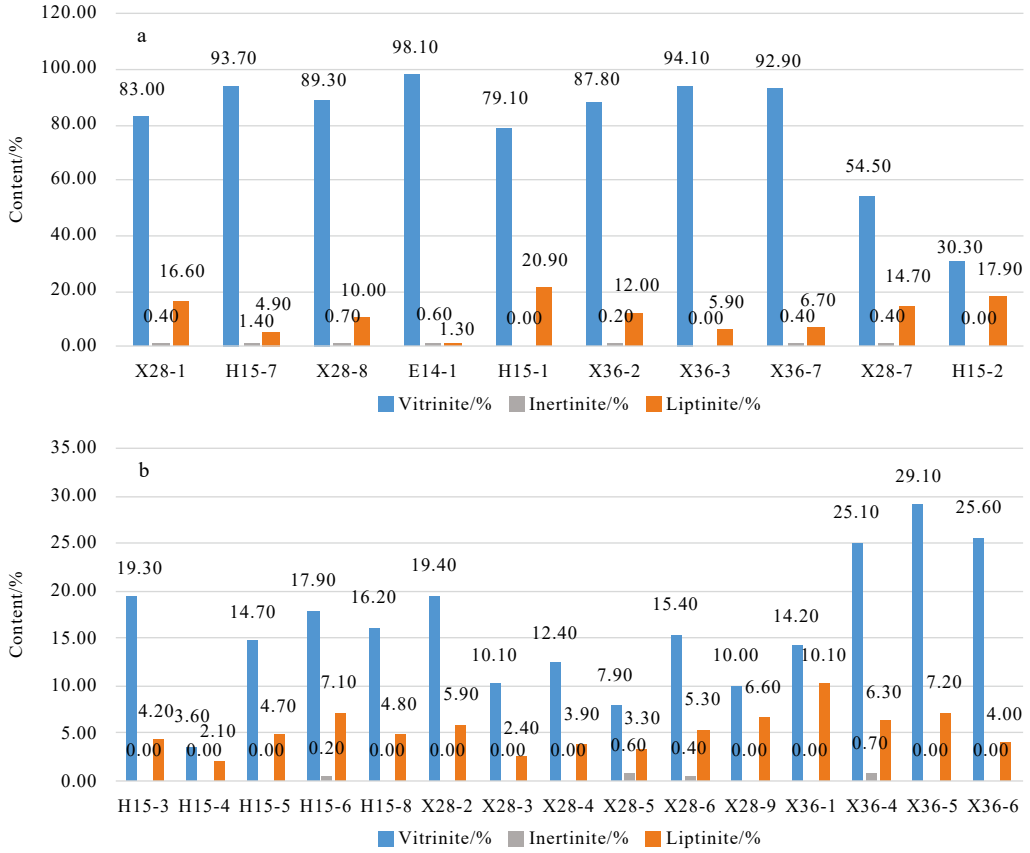

Fig. 6. Types and contents of organic macerals of Enping Formation the coal-measure source rock in Zhu Ⅰ Depression. a. Types and contents of organic macerals of Enping Formation coal in Zhu Ⅰ Depression; b. Types and contents of organic macerals in carbonaceous mudstones of Enping Formation in Zhu Ⅰ Depression

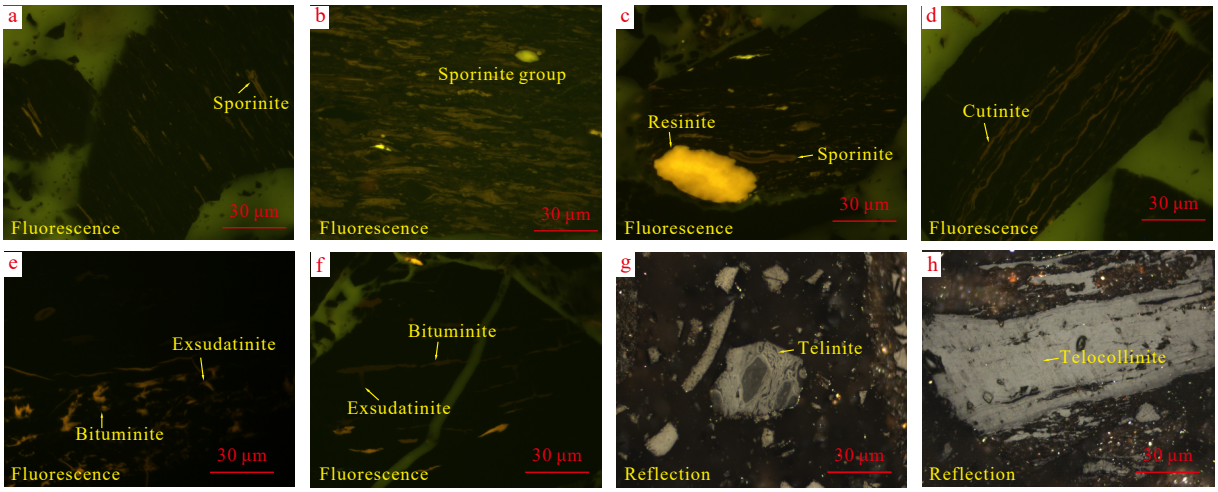

Fig. 7. Coal rock macerals of Enping Formation in Zhu Ⅰ Depression. a. Sporinite; b. Sporinite group; c. Resinite, Sporinite; d. Cutinit; e, f. Bituminite, Exsudatinite; g. Telinite; h. Telocollinite.

from 30.30%–98.10%, with an average of 80.30%. The liptinite content ranges from 1.30%-20.90%, with an average of 11.10%. The inertinite content ranges from 0–1.40%, with an average of 0.41% (Figs 6a and 7). In charcoal mudstone (15 samples), the vitrinite content ranges from 3.60%–29.10%, with an average of 16.10%, while the 5.20%, with the inertinite content ranging from 0–0.70%, with an average of 0.10% (Figs 6b and 7).

Macerals in coal rocks are the basic hydrocarbon generating units of source rocks, and different macerals have different hydrocarbon generating abilities (Tissot and Welte, 1984; Guo and Bustin, 1998; Sykes and Snowdon, 2002; Wilkins and George, 2002). Therefore, maceral is also an important index for evaluating the hydrocarbon generation potential of the coal-measure source rock. The differences in sedimentary environments affect the development of coal-forming plants, the types of peatification, and the preservation conditions of organic matter, resulting in significant differences and regularities in the macerals of the coal-measure source rock formed in different sedimentary envir-

onments.

(1) The coal-measure source rock in the braided river delta upper plain: The average maceral content in coal is 92.52%. The average vitrinite content is 61.54%, and the average liptinite content is 20.24% (Table 3). The average content of macerals in charcoal mudstone is 17.40%, while the average vitrinite content is 13.04%, and the average liptinite content is 4.16% (Table 3). The organic matter abundance, vitrinite, and liptinite contents are relatively high (Fig. 8).

(2) The coal-measure source rock in the braided river delta lower plain-braided river delta front: The average content of macerals in coal is 71.36%. The average vitrinite content is 51.39%, and the average liptinite content is 16.49% (Table 3). The average content of macerals in charcoal mudstone is 18.73%, while the average vitrinite content is 13.78%, and the average liptinite content is 4.92% (Table 3). The organic matter abundance, vitrinite, and liptinite contents are at a medium level (Fig. 8).

(3) The coal-measure source rock in the shore-shallow lake: The average maceral content in coal is 33.70%. The average vitrinite content is 26.60%, and the average liptinite is 6.75% (Table 3). The average maceral content in charcoal mudstone is 26.95%. The average vitrinite content is 19.90%, and the average liptinite content is 7.05% (Table 3). The organic matter abundance, vitrinite, and liptinite contents are relatively low (Fig. 8).

According to the study by Thompson et al. (1985), oil can be generated when the content of liptinite in the coal-measure source rock reaches 2%. The average content of liptinite in all the coal-measure source rock samples of the Enping Formation in Zhu Ⅰ Depression is 11.09%, which is much larger than 2% (Fig. 8), indicating good potential for oil production.

The concept of VI-GWI was proposed by Calder et al., 1991. Based on the relationship between grandwater influence (GWI) and vegetation index (VI), swamps can be divided into low peat swamps (VI < 3.0, 1.0 < GWI < 5.0), median peat swamps (VI < 4.0, 0.5 < GWI < 1.0), and high peat swamps (VI < 4.0, GWI < 0.5). The VI is calculated as follows:

$$\mathrm{VI}=\frac{\text{Telinite}+\text{Fusinite}+\text{Semifusinite}+\text{Suberinite}+\text{Resinite}}{\text{Vitrodetrinite}+\text{Liptodetrinite}+\text{Inertodetrinite}+\text{Alginite}+\text{Sporinite+Cutinite}}. \tag{1}$$

GWI is calculated as follows:

$$\mathrm{GWI}=\frac{\text{Gelocollinite}+\text{Corpogelinite}+\text{Vitrodetrinite}+\text{mineral}}{\text{Telinite}+\text{Telocollinite}+\text{Desmocollinite}}. \tag{2}$$

Most of the VI values in the study area are less than 1, indicating the dominance of herbaceous plants, with only a small part having VI values greater than 1, mainly representing woody plants. Similarly, most of the GWI values are less than 1 (Table 4),

Table 3. Maceral data of charcoal coal-measure source rock of Enping Formation in Zhu Ⅰ Depression

Sedimentary facies	Rockc characters	Liptinite/%	Vitrinite/%	Inertinite/%	Organic component fraction/%
Braided river delta upper plain	coal	20.24	61.54	10.74	92.52
	mudstone	(2.40–5.90)/4.16 (5)	(7.90–19.4)/13.04 (5)	(0.00–0.60)/0.20 (5)	(11.80–25.30)/17.40 (5)
Braided river delta lower plain-braided river delta front	coal	(6.00–40.00)/16.49 (7)	(30.30–81.00)/51.39 (7)	(0.00–9.76)/3.51 (7)	(45.60–90.00)/71.36 (7)
	mudstone	(2.10–7.10)/4.92 (6)	(3.60–19.30)/13.78 (6)	(0.00–0.20)/0.03 (6)	(5.70–25.20)/18.73 (6)
Shore-shallow lake	coal	(6.30–7.20)/6.75 (2)	(25.10–28.10)/26.60 (2)	(0.00–0.70)/0.35 (2)	(32.10–35.30)/33.70 (2)
	mudstone	(4.00–10.10)/7.05 (2)	(14.20–25.60)/19.90 (2)	(0.00–0.00)/0.00 (2)	(24.30–29.60)/26.95 (2)

Note: (6–40)/16.49 (7) is (min-max)/AVG (the No. of samples)

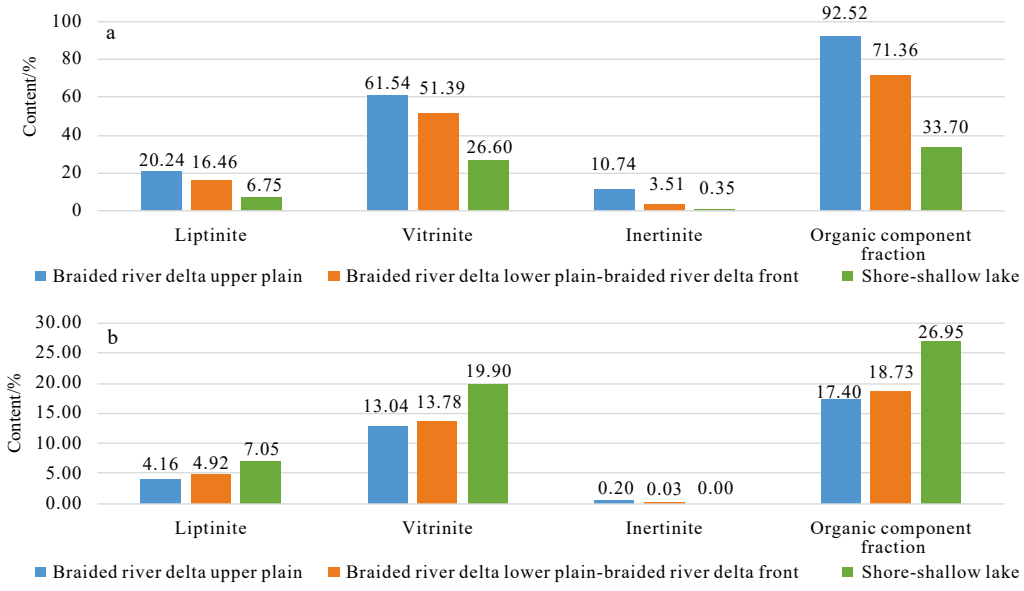

Fig. 8. Maceral content of the coal-measure source rock of Enping Formation in Zhu Ⅰ Depression. a. Maceral content of coal of Enping Formation in Zhu Ⅰ Depression; b. Maceral content of charcoal mudstone of Enping Formation in Zhu Ⅰ Depression.

Table 4. Maceral content and coal facies parameters of Paleogene Enping Formation coal in Zhu Ⅰ Depression, the Pearl (Zhujiang) River Mouth Basin

Coal facies	Well	T	Tl	Dl	Cg	Vd	Sf	TPI	GI	VI	GWI
Dry forest swamp	H15	0.00	17.40	10.90	0.00	2.00	0.00	1.35	0.63	0.04	1.99
		12.40	46.00	32.40	0.80	2.30	0.80	1.71	0.57	2.09	0.13
	X28	0.00	32.40	17.00	0.00	5.00	0.40	1.49	0.52	0.06	0.72
		3.40	45.20	37.60	0.90	2.20	0.00	1.22	0.79	0.37	0.26
	E14	10.90	41.30	42.10	0.60	3.30	0.60	1.16	0.9	2.50	0.07
AVG		5.34	36.46	28.00	0.46	2.96	0.36	1.39	0.68	1.01	0.63
Forest edge-wetland herbaceous swamp	X36	16.00	5.60	57.80	6.20	2.30	0.00	0.36	2.96	1.34	0.60
		2.50	34.20	54.60	1.10	1.80	0.00	0.65	1.52	0.39	0.60
	H15	12.00	17.60	61.40	1.90	0.00	0.40	0.49	2.14	2.34	0.59
		23.90	8.90	29.20	2.40	14.70	0.00	0.75	0.96	0.72	1.20
AVG		13.60	16.58	50.75	2.90	4.70	0.10	0.56	1.90	1.20	0.75
Open water swamp	X28	7.20	5.20	68.40	2.20	0.00	0.00	0.18	5.69	0.47	0.24

Note: T: Telinite; Tl: Telocollinite; Dl: Desmocollinite; Cg: Corpogelinite; Vd: Vitrodetrinite; Sf: Semifusinite; Ma: Macrinite; Id: Inertodetrinite.

indicating a predominantly medium peat swamp to high peat swamp environment.

Based on the gelatification index (GI) and tissue preservation index (TPI) proposed by Diessel (1986), the coal facies analysis diagram is constructed using single logarithmic coordinates. The coal facies parameters are calculated using the following formulas to analyze the coal-forming microenvironment.

Lu et al., (2014) put forward:

$$\mathrm{GI} = \frac{\text{Desmocollinite} + \text{Corpogelinite} + \text{Gelocollinite}}{\text{Telinite} + \text{Telocollinite}}. \tag{3}$$

Mao et al., (2011) put forward:

$$\mathrm{TPI} = \frac{\text{Telinite} + \text{Telocollinite} + \text{Semifusinite+Fusinite}}{\text{Desmocollinite} + \text{Vitrodetrinite} + \text{Macrinite} + \text{Inertodetrinite}}. \tag{4}$$

Gelatification index reflects the degree of water coverage of the peat swamp, with a higher GI indicating a relatively high groundwater level and wetter conditions. Tissue preservation index reflects the proportion of woody plants and herbaceous plants in the original coal-forming plants and can also indicate the pH value of the coal-forming environment to some extent. A low pH value inhibits bacterial activity, resulting in better preservation of plant material and higher TPI values (Tang et al., 2020).

The TPI value of Enping Formation coal in the Zhu Ⅰ Depression is relatively high, mostly around 1.00, and can reach a maximum of 1.49. This indicates well-preserved plants, a low pH value, and inhibited bacterial activity in a weakly acidic environment. Most of the GI values are less than 5, indicating a shallow and relatively dry environment overall (Table 4).

Three coal facies types, namely, dry forest swamp, forest edge-wetland herbaceous swamp, and open water swamp are identified in the Enping Formation of the Zhu Ⅰ Depression (Fig. 9).

(1) Dry forest swamp: GI < 1, TPI > 1. This facie type indicates a shallow water cover and a periodic dry swamp environment with weak hydrodynamic conditions. The swamp is located near the diving surface (Shen, 2018). Water flow in the environment is weak, resulting in stagnant water bodies (Wang and Tang, 2007). Coal seams are often developed in peat swamps on the braided river delta upper plain. The content of telocollinite is the highest, with an average of 36.46%. Desmocollinite follows with an average of 28.00%. The content of semifusinite is very small, with an average of 0.36%, without fusinite and macrinite (Table 4).

(2) Forest edge-wetland herbaceous swamp: GI < 5, TPI < 1. This facies type indicates a moderate water level, often extremely wet conditions dominated by sedge and wet gramineous plants, which are mostly perennial. Many plants have rhizomes and often form clusters. Coal seams are generally developed in the braided river delta lower plain swamp-interdistributary bay of braided river delta front. The content of desmocollinite is the highest, with an average of 50.75%, followed by telocollinite, with an average of 16.58%. The content of semifusinite is very small, with an average of 0.10%, without fusinite and macrinite (Table 4).

(3) Open water swamp: GI > 5, TPI < 1. This facies type indicates a deeper water cover and a swamp environment formed under weak hydrodynamic conditions, characterized by stagnant water bodies with weaker mobility (Wang and Tang, 2007). It is significantly influenced by periodic lake water, resulting in the development of many thin coal layers. Open water swamp is generally found in shore swamp environments. The content of desmocollinite is the highest, with an average of 68.40%, fol-

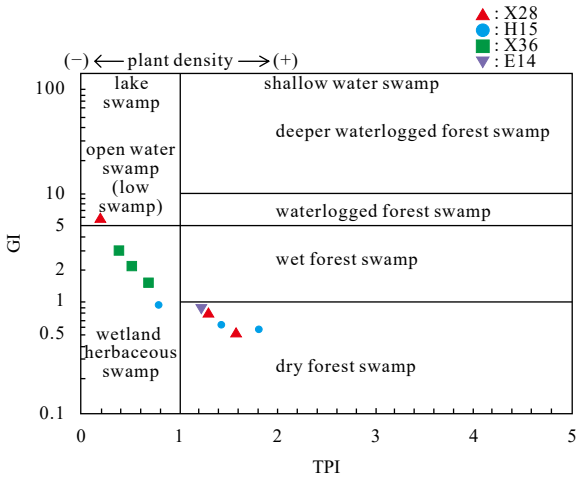

Fig. 9. Coal facies classification of Enping Formation in Zhu Ⅰ Depression.

lowed by telocollinite, with an average of 5.20%, without semi-fusinite, fusinite, or macrinite (Table 4).

Additionally, some trace elements can indicate the palaeoenvironment. V/(V+Ni) is commonly used as an indicator of paleo-oxygenation facies. V/(V+Ni) > 0.84 indicates an oxygen-deficient environment, 0.60 < V/(V+Ni) < 0.84 indicates a weak oxygen environment, and V/(V+Ni) < 0.46 indicates an oxygen rich environment (Liu and Zhou, 2007). Sr and Ba can be used as indicator elements to determine the salinity of paleo-water bodies. The value of Sr/Ba in freshwater sediments is usually less than 0.6, while in saline water environments, it is greater than 1.0. Values between 0.6 and 1.0 represent brackish water transition environments (Deng and Qian, 1993; Zheng and Liu, 1999).

The average value of V/(V+Ni) in the study area is 0.80-0.82, indicating a weakly oxidized environment. The average value of Sr/Ba is 0.17–0.33, which is less than 0.60 overall, indicating low salinity and a freshwater environment (Table 1).

Biomarkers also provide indications of the paleoenvironment. The Pr/Ph value of the coal-measure source rock in the Enping Formation of the Zhu Ⅰ Depression is generally > 1 (Table 5), suggesting a partially oxidized environment with relatively shallow water bodies. The relationship diagram of Pr/nC$_{17}$–Ph/nC$_{18}$ also supports the presence of a partially oxidized environment in the coal-measure source rock of Enping Formation (Fig. 10).

Table 5. Biomarker data table of Paleogene Enping Formation in Zhu I Depression

Well	CPI	OEP	$\sum nC_{21}^{-}/\sum nC_{22}^{+}$	Pr/nC$_{17}$	Ph/nC$_{18}$	Pr/Ph
H31	(1.84–3.34)/2.29 (8)	(0.26–3.31)/1.70(8)	(0.16–0.51)/0.30(8)	(0.35–1.89)/0.94(8)	(0.24–0.51)/0.37(8)	(0.54–3.89)/1.89(8)
H10	(1.00–1.21)/1.13(4)	(0.87–1.21)/1.06 (4)	(0.23–0.51)/0.40(4)	(0.84–4.66)/3.07(4)	(0.28–0.52)/0.40(4)	(0.47–8.34)/5.11(4)
H26	1.08	1.02	0.67	1.11	0.17	5.81
X36	(1.09–1.39)/1.24 (2)	(1.07–1.50)/1.29(2)	(0.26–0.83)/0.55(2)	(0.42–4.27)/2.35(2)	(0.21–1.06)/0.64(2)	(1.95–4.19)/3.07(2)

Note: (1.84 – 3.3)/2.29 (8) is (min -max)/AVG (the No. of samples); CPI = 1/2[($\sum C_{25} - C_{33}$)/($\sum C_{24} - C_{32}$) + ($\sum C_{25} - C_{33}$)/($\sum C_{26} - C_{34}$)]; OEP = ($C_{25} + 6C_{27} + C_{29}$)/($4C_{26} + 4C_{28}$); $\sum nC_{21}^{-}/\sum nC_{22}^{+}$: low carbon number/high carbon number; Pr/Ph: Pristane/Phytane.

In summary, the coal-measure source rock in the Enping Formation of the Zhu Ⅰ Depression developed in a weakly oxidized freshwater environment with shallow water depth.

4 Analysis of the hydrocarbon generation potential of the coal-measure source rock in the Enping Formation

4.1 *Organic matter abundance of the coal-measure source rock in the Enping Formation*

The abundance of organic matter is usually reflected by the content of TOC and chloroform bitumen "A" (Tissot and Welte, 1984; Pepper and Corvi, 1995). The content of chloroform bitumen "A" is numerically equal to that of S_1 (Liu, 2009). Therefore, the content of S_1 is used to represent the content of chloroform bitumen "A".

According to the criterion proposed by Chen et al. (1997) for evaluating the coal-measure source rock, the organic matter abundance of the coal-measure source rock formed in different sedimentary environments of the Enping Formation in the Zhu Ⅰ Depression exhibits certain regularity and differences (Table 6).

(1) The Coal-Measure Source Rock in the braided river delta upper plain: The average TOC content in coal is 65.21%, and the average content of chloroform bitumen "A" is 9.39 mg/g. The average TOC content of charcoal mudstone is 11.82%, and the average content of chloroform bitumen "A" is 1.16 mg/g. The abundance of organic matter is relatively high.

(2) The Coal-Measure Source Rock in the braided river delta lower plain-braided river delta front: The average TOC content in coal is 47.01%, and the average content of chloroform bitumen "A" is 12.07 mg/g. The average TOC content of charcoal mudstone is 11.26%, and the average content of chloroform bitumen "A" is 2.27 mg/g. The abundance of organic matter is at a moderate level.

(3) The Coal-Measure Source Rock in the Shore-shallow lake: The average content of TOC in coal is 42.59%, and the average content of chloroform bitumen "A" is 5.97 mg/g. The average TOC content of charcoal mudstone is 13.05%, and the average content of chloroform bitumen "A" is 2.21 mg/g. The abundance of organic matter is relatively low.

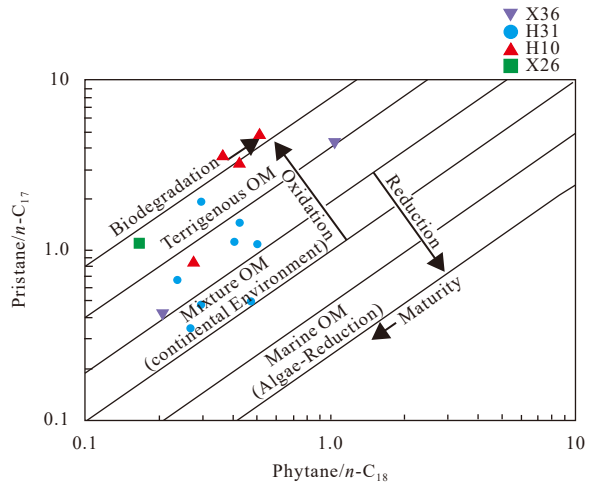

Fig. 10. Ph/nC$_{18}$-Pr/nC$_{17}$ diagram of Enping Formation in Zhu I Depression.

4.2 *Types of organic matter in the coal-measure source rock of the enping formation*

Kerogen, according to the source of sedimentary organic matter and its different hydrocarbon generation abilities, can be divided into three types: type Ⅰ, type Ⅱ, and type Ⅲ (Peters and Cassa, 1994; Vandenbroucke and Largeau, 2007).

By examining the relationship between Pr/nC$_{17}$ and Ph/nC$_{18}$ (Fig. 10), it can be observed that the organic matter of the coal-measure source rock in the Enping Formation of the Zhu I Depression is mainly derived from terrestrial and mixed biological sources. The value of the CPI is generally > 1, showing an odd carbon number predominance and reflecting the source of organic matter from terrestrial higher plants. The value of $\sum nC_{21}^{-}/\sum nC_{22}^{+}$ is small, which also reflects the source of terrestrial higher plants (Table 5). All these findings indicate that the organic matter type of the coal-measure source rock in Enping Formation is mainly type Ⅱ kerogen.

Rock pyrolysis is an effective method for determining the type of organic matter. In this study, the T_{max}-HI evaluation diagram is

used for this purpose. Additionally, Peters et al. (1993) point out that the coal-measure source rock with a hydrogen index greater than 300 mg/g.(TOC) are oil-prone hydrocarbon source rocks, those with a hydrogen index of 200–300 mg/g.(TOC) are oil and gas-prone hydrocarbon source rocks, those with a hydrogen index of 50–200 mg/g.(TOC) are gas-prone hydrocarbon source rocks, and those with a hydrogen index less than 50.00 mg/g.(TOC) are non-hydrocarbon source rocks.

The organic matter types of coal in the braided river delta upper plain of the Paleogene Enping Formation in the Zhu Ⅰ Depression are primarily type Ⅱ$_1$ and type Ⅱ$_2$ (Fig. 11a), with an average HI of 231 mg/g.(TOC) (Table 6). The organic matter type of charcoal mudstone is mainly type Ⅱ$_1$ with a small amount of type Ⅱ$_2$ (Fig. 11b), with an average HI of 250.75 mg/g.(TOC) (Table 6). They belong to oil and gas-prone hydrocarbon source rocks with relatively high oil-proneness.

The organic matter types of coal in thebraided river delta lower plain-braided river delta front are mainly type Ⅱ$_1$, with a small amount of type Ⅱ$_2$ (Fig. 11a), with an average HI of 287.16 mg/g.(TOC) (Table 6). The organic matter type of charcoal mudstone is mainly type Ⅱ$_1$, with a small amount of type I and type Ⅱ$_2$ (Fig. 11b), with an average HI of 241.31 mg/g.(TOC) (Table 6). They belong to oil- and gas-prone hydrocarbon source rocks with a relatively moderate oil-proneness.

The shore-shallow lake's coal and charcoal mudstone contain predominantly type Ⅱ$_2$ organic matter, with a minor presence of type Ⅱ$_1$ (Fig. 11). The coal has an average HI of 216 mg/g.(TOC), while charcoal mudstone has an average HI of 178.50 mg/g.(TOC) (Table 6). The majority of these rocks are gas-prone hydrocarbon source rocks, while a minority are oil and gas-prone hydrocarbon source rocks with relatively poor oil-proneness.

The above findings indicate that the coal-measure source rock of the Paleogene Enping Formation in the Zhu Ⅰ Depression has good oil-proneness. Among them, the braided river delta upper plain exhibits relatively high oil-proneness, followed by the braided river delta lower plain-braided river delta front, while the shore-shallow lake shows relatively poor oil proneness.

4.3 *Organic matter maturity of the coal-measure source rock in the Enping Formation*

The generation and accumulation of oil and gas in hydrocarbon source rocks occur only when they reach a certain level of maturity. The maturity of organic matter is an important para-

Table 6. Geochemical data of the coal-measure source rock of Enping Formation in Zhu Ⅰ Depression

Sedimentary facies	Rockc characters	TOC/%	S_1/(mg·g^{-1})	S_1+S_2/(mg·g^{-1})	HI/(mg·g^{-1}·(TOC))
Braided river delta upper plain	coal	(47.91–77.53)/65.21(4)	(4.77–13.10)/9.39(4)	(130.48–199.05)/159.22(4)	(205–255)/231(4)
	mudstone	(7.30–19.61)/11.82(8)	(0.49–2.36)/1.16(8)	(15.40–66.48)/31.90(8)	(196–327)/250.75(8)
Braided river delta lower plain-braided river delta front	coal	(26.2–62.7)/47.01(7)	(2.15–25.92)/12.07(7)	(70.56–248.63)/152.14(7)	(182–356)/287.16(7)
	mudstone	(6.05–18.65)/11.26 (14)	(0.41–5.58)/2.27(14)	(16.44–48.30)/29.23(14)	(202–327)/241.31(14)
Shore-shallow lake	coal	(35.11–51.23)/42.59(3)	(5.11–7.63)/5.97(3)	(81.61–130.45)/98.51(3)	(185–240)/216(3)
	mudstone	(6.82–15.13)/13.05(4)	(1.67–2.94)/2.21(4)	(12.46–31.04)/26.11(4)	(147–192)/178.50(4)

Note: (47.91–77.53)/65.21 (4) is (min-max)/AVG (the No. of samples); HI: hydrogen index.

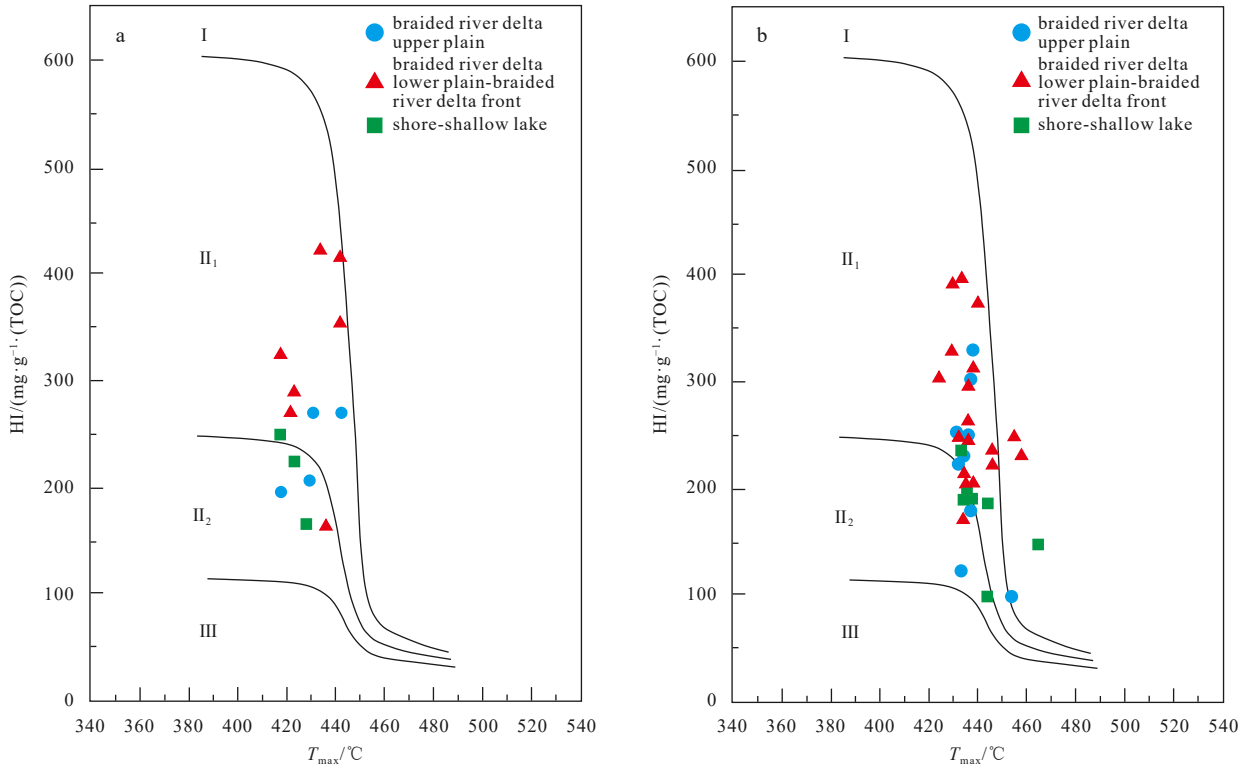

Fig. 11. Organic matter types of Paleogene coal measure source rocks in Zhu Ⅰ Depression. a. Organic matter types of Paleogene coal in Zhu Ⅰ Depression; b. organic matter types of paleogene charcoal mudstone in Zhu Ⅰ Depression.

meter for evaluating hydrocarbon source rocks as it reflects the degree of thermal evolution of kerogen.

Numerous studies have been conducted on the hydrocarbon generation threshold of Paleogene-Neogene coal in China. Some experts suggest that the hydrocarbon generation threshold of coal in the Xihu Sag of the East China Sea Shelf Basin starts at R^o_{max} = 0.55% (Li et al., 1997; Zhang, 2017), while others suggest a threshold of R^o_{max} = 0.5%. Based on the analysis of relevant data from the CNOOC Research Institute, it is considered that the hydrocarbon generation threshold of the coal-measure source rock in the Paleogene Enping Formation of the Zhu Ⅰ Depression is approximately R^o_{max} = 0.50%.

According to the Pr/nC_{17}-Ph/nC_{18} diagram (Fig. 10), it indicates that the organic matter of the coal-measure source rock in the Enping Formation is in the mature stage. Most of the OEP values are between 1.00 and 1.40, representing the low-high-mature stage (Table 5). The maximum vitrinite reflectance of the coal-measure source rock in the Enping Formation ranges mostly between 0.75%–1.30%, indicating a stage of extensive oil generation and high maturity. The T_{max} value of the coal-measure source rock in the Enping Formation ranges between 424–456℃, with most values around 435℃, representing a stage of low maturity and extensive oil generation, with some samples still in the immature stage (Table 7). Microscopic observations reveal the presence of exsudatinite, indicating the initiation of hydrocarbon generation (Figs 7e and f). Overall, the coal-measure source rock of the Paleogene Enping Formation in the Zhu Ⅰ Depression is in the stage of significant oil generation.

A positive correlation exixts between R^o_{max} and the burial depth of coal in the Enping Formation the coal-measure source rock (Fig. 12). The T_{max} value of charcoal mudstone also shows a positive correlation with the burial depth (Fig. 13), suggesting variations in thermal evolution with the depth for the the coal-measure source rock.

4.4 *Characteristics of the hydrocarbon generation potential of the coal-measure source rock in the Enping Formation*

The hydrocarbon generation potential of the hydrocarbon source rocks is an important parameter for characterizing their ability to generate hydrocarbon source rocks. S_1+ S_2 is the most commonly used index for assessing the hydrocarbon generation potential of hydrocarbon source rocks.

In the coal-measure source rock of the Paleogene Enping Formation in the Zhu Ⅰ Depression, the hydrocarbon generation potential of hydrocarbon source rocks formed in different sedimentary environments exhibits certain regularity and differences:

(1) The S_1+ S_2 value of coal in the braided river delta upper plain ranges between 130.48 mg/g to 199.05 mg/g, with an average of 159.22 mg/g. The S_1+ S_2 value of charcoal mudstone ranges between 15.40 mg/g to 66.48 mg/g, with an average of 31.90 mg/g (Table 6). The hydrocarbon generation potential of the coal-measure source rock is relatively high (Figs 14–17).

(2) The S_1+ S_2 value of coal in the braided river delta lower plain-braided river delta front ranges between 70.56–248.63 mg/g, with an average of 152.14 mg/g .The S_1+ S_2 value of charcoal mudstone ranges between 16.44 mg/g and 48.30 mg/g, with an average of 29.23 mg/g (Table 6). The hydrocarbon generation potential of the coal-measure source rock is at the middle level (Figs 14–17).

(3) The S_1+ S_2 value of coal in the shore-shallow lake ranges between 81.61–130.45 mg/g, with an average of 98.51 mg/g, while the S_1+ S_2 value of charcoal mudstone ranges between 12.46–31.04 mg/g, with an average of 26.11 mg/g (Table 6). The hydrocarbon generation potential of the coal-measure source rock is relatively lower (Figs 14-17).

The hydrocarbon generation potential of Paleogene Enping Formation coal in the Zhu Ⅰ Depression exhibits the strongest correlation with the content of organic components in coal (Fig. 18), followed by TOC content and vitrinite content (Fig. 19). The hydrocarbon generation potential of charcoal mudstone shows the strongest correlation with TOC content (Fig. 20), followed by liptinite content, while its correlation with organic component content and vitrinite content is the weakest (Fig. 21).

Previous oil-source correlation studies have been conducted to determine the contribution of the coal-measure source rock of the Enping Formation to the oil pool in this area (Ma et al., 1988). By comparing the Pr/Ph histograms of crude oil and source rock (Fig. 22), it can be observed that the source rocks of the Wenchang Formation and Enping Formation are similar to crude oil. Further comparison of the parent source parameters and maturity parameters of crude oil and source rock helps clarify the actual source rock. C_{27} sterane is dominant in the source rocks of the Wenchang Formation, with C_{29}/C_{27} < 1, while C_{29} sterane is dominant in the source rocks of the Enping Formation, with C_{29}/C_{27} between 1–3. The distribution range of crude oil parent source

Table 7. Maturity classification table of coal measure source rocks of Paleogene Enping Formation in Zhu Ⅰ Depression

Evolutionary phase	Immaturity	Low maturity–Large oil-generating	Large oil-generating–Highly maturity	Over-maturity	Dry gas stage
R^o_{max}/%	<0.5	0.5–0.75	0.75–1.30	1.3–2	>20
T_{max}/℃	<435	435–480	480–510	>510	>510

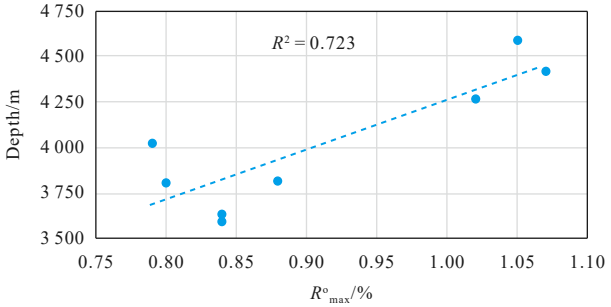

Fig. 12. Relationship between R^o_{max} and buried depth of Enping Formation coal in Zhu Ⅰ Depression

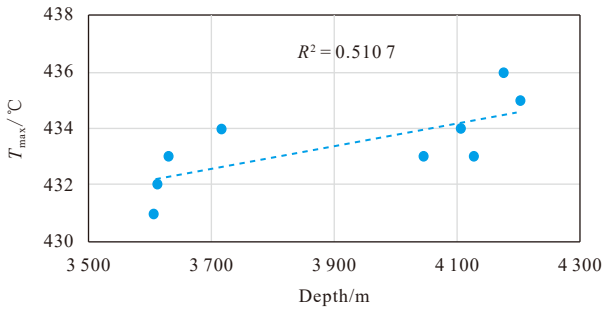

Fig. 13. Relationship between T_{max} and buried depth of charcoal mudstone in Enping Formation of Zhu Ⅰ Depression

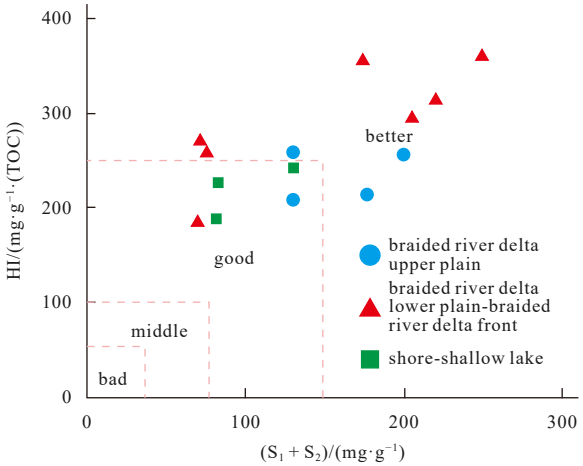

Fig. 14. (S_1+S_2)-HI diagram of coal in Enping Formation.

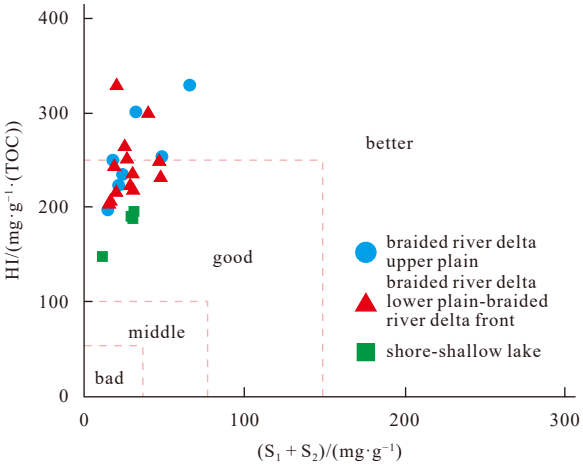

Fig. 15. (S_1+S_2)-HI diagram of charcoal mudstone in Enping Formation.

parameter values aligns exactly with that of the Wenchang Formation and Enping Formation, confirming that they are oil source rocks. This oil-source correlation demonstrates that the coal-measure source rock of the Enping Formation is one of the significant oil pool source rocks in this area.

5 Sedimentary organic facies and grade rating of the coal-measure source rock in the Enping Formation

Based on the above analysis of organic matter abundance, organic matter maturity, organic matter type, and the hydrocarbon generation potential of the coal-measure source rock in the Enping Formation, the sedimentary organic facies characteristics of the Paleogene Enping Formation coal-measure source rock in the Zhu Ⅰ Depression are summarized as follows, according to the standard proposed by the Chen et al. (1997). The quality grade of the coal-measure source rock in the Paleogene Enping Formation of the Zhu Ⅰ Depression is comprehensively evaluated (Table 8).

(1) Upper plain swamp-dry forest swamp facies: located above the diving surface. The content of organic components is higher, among which the content of vitrinite is higher and mainly telocollinite, and the content of liptinite is higher, mainly sporinite and cutinite, GI < 1, TP I > 1, it shows that the water is shallow and the plants are preserved intact. The coal-measure source

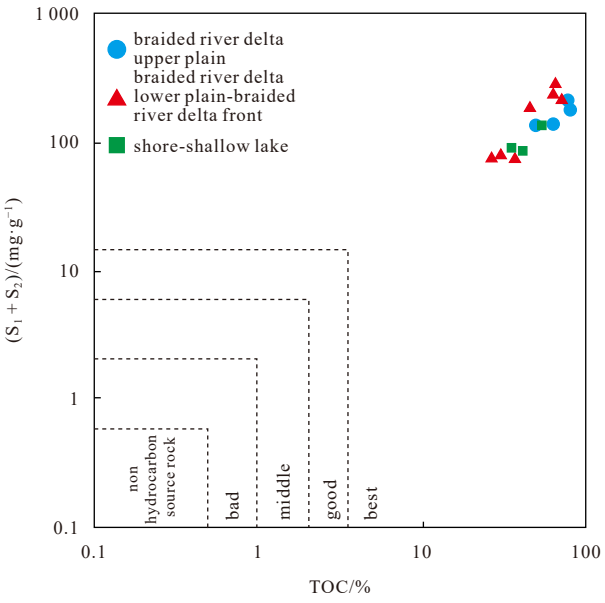

Fig. 16. TOC-(S_1+S_2) diagram of coal in Enping Formation.

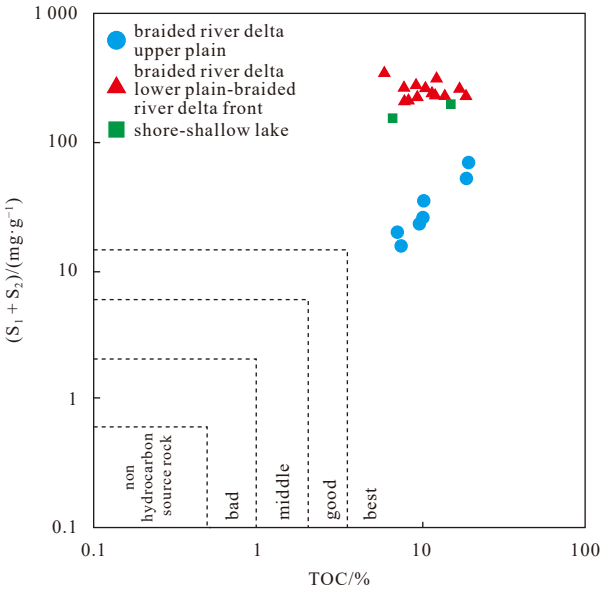

Fig. 17. TOC-(S_1+S_2) diagram of charcoal mudstone in Enping Formation.

rock formed by this kind of sedimentary organic facies have relatively good hydrocarbon generation potential and relatively high oil-prone, and most of them belong to good-best hydrocarbon source rock. This is mainly because the braided river delta upper plain is not deep in water and rich in nutrients, which is conducive to the growth and accumulation of plants, at the same time, the sedimentary environment is relatively stable, which is conducive to the formation of coal seams.

(2) Lower plain-interdistributary bay-forest-herbaceous swamp facies: located below the diving surface. The content of organic components is middle, among which the content of vitrinite is middle and mainly desmocollinite, and the content of liptinite is middle, mainly sporinite and cutinite, GI < 5, TPI < 1, it shows that the overlying water is at a medium level, and the plants are relatively poorly preserved. The coal-measure source

Table 8. The sedimentary organic facies of the coal-measure source rock of the Paleogene Enping Formation in Zhu Ⅰ Depression, the Pearl (Zhujiang) River Mouth Basin

Sedimentary organic facies	Upper Plain Swamp-Dry Forest Swamp Facies	Lower Plain-Interdistributary Bay-Forest-Herbaceous Swamp Facies	Lake Swamp-Herbaceous Swamp Facies
Coal facies	Dry Forest Swamp	Forest Edge-Wetland Herbaceous Swamp	Open water swamp
Sedimentary systems	Braided river delta upper plain	Braided river delta lower plain-braided river delta front	Shore-shallow lake
Microscopic composition	vitrinite is dominated by telocollinite; liptinite is dominated by cutinite and sporinite	vitrinite is dominated by desmocollinite; liptinite is dominated by cutinite and sporinite	vitrinite is dominated by desmocollinite; liptinite is dominated by cutinite and sporinite
Microscopic mark	GI < 1, TPI > 1	GI < 5, TPI < 1	GI > 5, TPI < 1
Hydrodynamic conditions	Above the diving surface	Below the diving surface	Flowing water underwater deposition
Organic matter type	Coal: Ⅱ$_1$, Ⅱ$_2$ type; Charcoal mudstone: type Ⅱ$_1$ is the main type, a small amount of type Ⅱ$_2$.	Coal: type Ⅱ$_1$ is the main type, a small amount of type Ⅱ$_2$; Charcoal mudstone: type Ⅱ$_1$ is the main type, a small amount of type Ⅰ and type Ⅱ$_2$	Coal: type Ⅱ$_2$ is the main type, a small amount of type Ⅱ$_1$; Charcoal mudstone: type Ⅱ$_2$ is the main type, a small amount of type Ⅱ$_1$
Geochemical feature	Coal: S_1+S_2: $\frac{130.48-199.05\ mg/g}{159.22\ mg/g}$ HI: $\frac{205-255\ mg/g(TOC)}{231\ mg/g(TOC)}$ Charcoal mudstone: S_1+S_2: $\frac{15.4-66.48\ mg/g}{31.90\ mg/g}$ HI: $\frac{196.00-327.00\ mg/g(TOC)}{250.75\ mg/g(TOC)}$	Coal: S_1+S_2: $\frac{70.56-248.63\ mg/g}{152.14\ mg/g}$ HI: $\frac{182.00-356.00\ mg/g(TOC)}{287.16\ mg/g(TOC)}$ Charcoal mudstone: S_1+S_2: $\frac{16.44-48.30\ mg/g}{29.23\ mg/g}$ HI: $\frac{202.00-327.00\ mg/g(TOC)}{241.31\ mg/g(TOC)}$	Coal: S_1+S_2: $\frac{81.61-130.45\ mg/g}{98.51\ mg/g}$ HI: $\frac{185.00-240.00\ mg/g(TOC)}{216.00\ mg/g(TOC)}$ Charcoal mudstone: S_1+S_2: $\frac{12.46-31.04\ mg/g}{26.11\ mg/g}$ HI: $\frac{47.00-192.00\ mg/g(TOC)}{178.50\ mg/g(TOC)}$
Hydrocarbon generation potential	High hydrocarbon generation potential	Medium hydrocarbon generation potential	Low hydrocarbon generation potential
Oil producibility	Large oil-generating	Large oil-generating	Large oil-generating

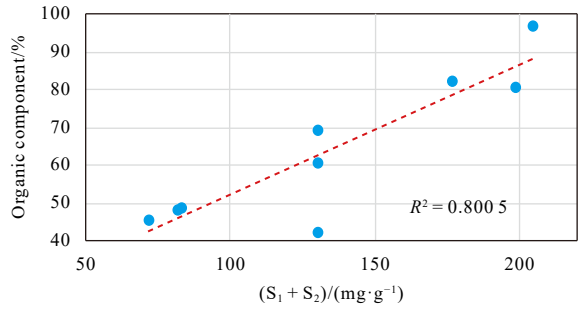

Fig. 18. The relationship between organic component content and S_1+S_2 of coal in Enping Formation.

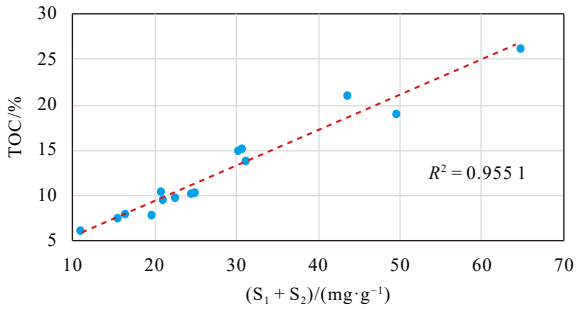

Fig. 20. The relationship between TOC and S_1+S_2 of charcoal mudstone in Enping Formation.

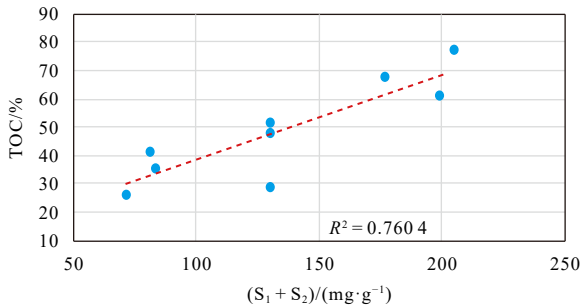

Fig. 19. The relationship between TOC and S_1+S_2 of coal in Enping Formation.

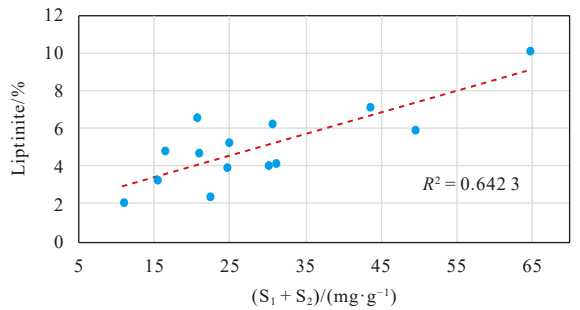

Fig. 21. The relationship between Liptinite group and S_1+S_2 of charcoal mudstone in Enping Formation.

rock formed by this kind of sedimentary organic facies have relatively middle hydrocarbon generation potential and relatively middle oil-prone, and most of them belong to good-best hydrocarbon source rock. This is mainly because the braided river delta lower plain-braided river delta front is significantly affected by the lake water, and the sedimentary environment is unstable, resulting in a small thickness of the coal seam.

(3) Lake swamp-herbaceous swamp facies: It belongs to underwater deposition of running water. The content of organic components is lower, among which the content of vitrinite is

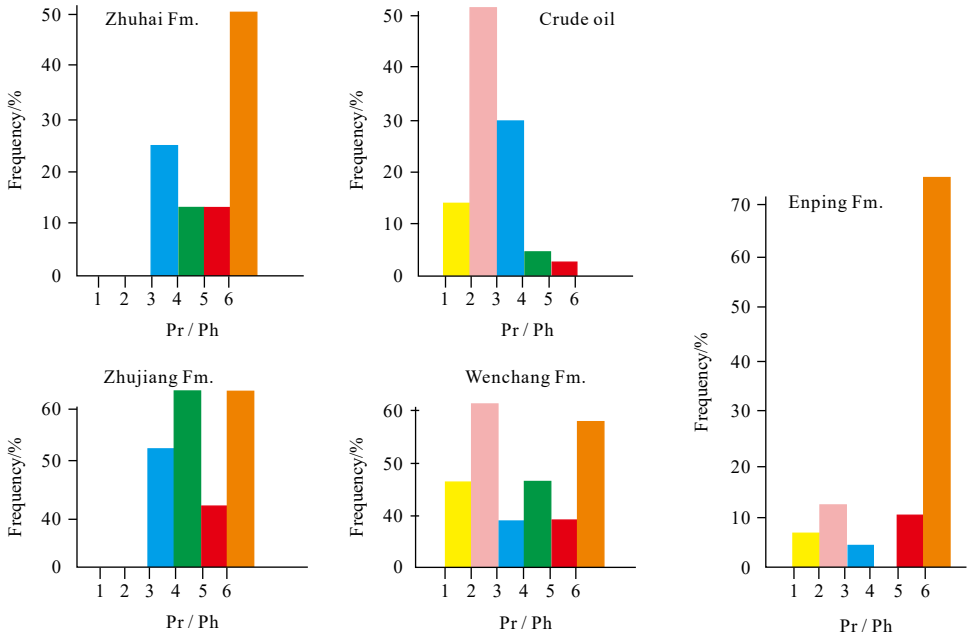

Fig. 22. Pr/Ph value frequency histogram of crude oil and source rock in Pearl (Zhujiang) River Mouth Basin (modified from Ma et al., 1988).

lower and mainly desmocollinite, and the content of liptinite is lower, mainly sporinite and cutinite, GI > 5, TPI < 1, it shows that the water is deep and the plant preservation is relatively poor. The coal-measure source rock formed by this kind of sedimentary organic facies have relatively worse hydrocarbon generation potential and relatively worse oil-prone, and most of them belong to good hydrocarbon source rock. This is mainly because the coal seam is destroyed due to the frequent water intake and retreat during the deposition of coal seam, which is not conducive to the formation of thick coal seam.

6 Conclusion

(1) The Paleogene Enping Formation in the Zhu Ⅰ Depression represents a typical combination of *Dicolpopllos kockolii* and *Gothanipollis bassensis*. The sporopollen characteristics indicate a tropical-subtropical climate for the Enping Formation. The coal-measure source rock of the Enping Formation developed in a warm, wet, and weakly oxidized fresh water environment.

(2) The main coal-forming environments of the Enping Formation include the peat swamp in the braided river delta upper plain with thick coal seams. The braided river delta lower plain swamp-interdistributary bay of braided river delta front greatly affected by the intake and retreat of lake water, resulting in many coal layers, small thickness, and poor stability. The shore swamp controlled by frequent fluctuations in lake water, with many coal layers and thin thickness.

(3) The organic matter abundance in the coal-measure source rock of the Enping Formation is highest in the braided river delta upper plain, followed by the braided river delta lower plain-braided river delta front, and lowest in the shore-shallow lake. The dominant organic matter type is type Ⅱ$_1$, with a higher HI, indicating a clear tendency for oil generation. The R^o_{max} and T_{max} values indicate that the coal-measure source rock is approaching the stage of extensive oil generation.

(4) The hydrocarbon generation potential of the coal-measure source rock in the Enping Formation is generally high, with the braided river delta upper plain having the highest hydrocarbon generation potential, followed by the braided river delta lower plain-braided river delta front, and the shore-shallow lake having the lowest. The hydrocarbon generation potential shows the strongest correlation with the content of organic components in coal, while the hydrocarbon generation potential of charcoal mudstone shows the strongest correlation with TOC content.

(5) Three types of sedimentary organic facies are identified in the coal-measure source rock of the Paleogene Enping Formation in the Zhu Ⅰ Depression. The upper plain swamp-dry forest swamp facies located above the diving surface with shallow water cover, intact plants and good hydrocarbon generation potential. Most of them belongs to good-to-best hydrocarbon source rocks. The lower plain-interdistributary bay-forest-herbaceous swamp facies located below the diving surface with the overlying water at a medium level. Plant preservation is relatively poor. The hydrocarbon generation potential is also moderate, and most of them belong to the good to best hydrocarbon source rocks. The lake swamp-herbaceousswamp facies resulted from subaqueous deposition by flowing water. The overlying water is relatively deep, and plant preservation is relatively poor. The hydrocarbon generation potential is relatively low. Overall, it belongs to a good hydrocarbon source rock.

Acknowlegements

Thank you for the professional support and data support provided by the relevant experts of CNOOC Research Institute, and thank you to all the experts who have helped me. Finally thank the reviewers for their opinions.

References

Calder J H, Gibling M R, Mukhopadhyay P K. 1991. Peat formation in a Westphalian B piedmont setting, Cumberland Basin, Nova Scotia; implications for the maceral-based interpretation of rheotrophic and raised paleomires. Bulletin de la Societe Geologique de France, 162(2): 283–298

Chen Jianping, Zhao Changyi, He Zhonghua. 1997. Criteria for evaluating the hydrocarbon generating potential of organic matter in

coal measures. Petroleum Exploration and Development (in Chinese), 24(1): 1–5
China National Offshore Oil Corporation. 2007. Study on Paleogene biostratigraphy in eastern Pearl River Estuary Basin. (in Chinese) Beijing: Beijing Research Center of China National Offshore Oil Corporation
Dai Shifeng, Bechtel A, Eble C F, et al. 2020. Recognition of peat depositional environments in coal: A review. International Journal of Coal Geology, 219: 103383, doi: 10.1016/j.coal.2019.103383
Deng Mingfang, Chen Weihuang. 1989. Geologic settings for YA 13–1 giant gas field formation. China Offshore Oil and Gas (Geology) (in Chinese), 3(6): 19–26
Deng Yunhua, Lan Lei, Li Youchuan, et al. 2019. On the control effect of deltas on the distribution of marine oil and gas fields in the South China Sea. Acta Petrolei Sinica (in Chinese), 40(S2): 1–12
Deng Hongwen, Qian Kai. 1993. Sedimentary Geochemistry and Environmental Analysis (in Chinese). Lanzhou: Science Technique Press, Gansu: 4–31
Diessel C F K. 1987. On the correlation between coal facies and depositional environments. In: 20th Symposium of the Advances in the Study of the Sydney Basin. Newcastle, Australia: 19–22
Ding Lin, Li Xiaoyan, Zhou Fengjuan, et al. 2022. Differential development characteristics and main controlling factors of the Paleogene high-quality reservoirs from the Zhu Ⅰ Depression in the Pearl River Mouth Basin: A case on Wenchang Formation at Lufeng area and Huizhou area. Acta Petrologica et Mineralogica (in Chinese), 41(1): 75–86
Fu Ning, Deng Yunhua, Zhang Gongcheng, et al. 2010. Transitional source rock and its contribution to hydrocarbon accumulation in superimpose rift-subsidence basin of northern South China Sea: Taking Baiyun Sag of Zhu Ⅱ Depression as an example. Acta Petrolei Sinica (in Chinese), 31(4): 559–565
Gao Yangdong, Lin Heming, Wang Xudong, et al. 2022. Geochemical constraints on the cedimentary environment of Wenchang Formation in Pearl River Mouth Basin and its paleoenvironmental implications. Geoscience (in Chinese), 36(1): 118–129
Guo Pengfei. 2015. Formation mechanism of high-quality source rock and its contribution to hydrocarbon accumulation in Zhuyi Depression, Pearl River Mouth Basin (in Chinese) [dissertation]. Wuhan: China University of Geosciences
Guo Yingting, Bustin R M. 1998. Micro-FTIR Spectroscopy of liptinite Macerals in coal. International Journal of Coal Geology, 36(3-4): 259–275, doi: 10.1016/S0166-5162(97)00044-X
Han Meilian, Wei Jiuchuan. 2001. Deltaic depositional system and coal-accumulation in Juye Coalfield. Acta Sedimentologica Sinica (in Chinese), 19(3): 381–385
Huang Baojia, Wang Zhenfeng, Liang Gang. 2014. Natural gas source and migration-accumulation pattern in the central canyon, the deep water area, Qiongdongnan basin. China Offshore Oil and Gas (in Chinese), 26(5): 8–14
Jiang Hua, Wang Hua, Li Junliang, et al. 2009. Research on hydrocarbon pooling and distribution patterns in the Zhu-3 Depression, the Pearl River Mouth Basin. Oil & Gas Geology (in Chinese), 30(3): 275–281,286
Kang Shilong, Shao Longyi, et al. 2020. Hydrocarbon generation potential and depositional setting of Eocene oil-prone coaly source rocks in the Xihu Sag, East China Sea shelf basin. ACS Omega, 5(50): 32267–32285, doi: 10.1021/acsomega.0c04109
Lermana. 1989. Chemical Geology and Physics of Lake (in Chinese). Beijing: Geological Publishing House, 197–236
Li Shaojie. 2015. Study on the formation modes of coal-measure source rocks in Northern basins of South China Sea (in Chinese) [dissertation]. Wuhan: China University of Geosciences
Li Youchuan, Deng Yunhua, Zhang Gongcheng. 2014. Gas-rich zone and main controlling factors of gas source rock in offshore China. Natural Gas Geoscience (in Chinese), 25(9): 1309–1319
Li Zengxue, He Yuping, Liu Haiyan, et al. 2010. Sedimentology characteristics and coal-forming models in Yacheng Formation of Qiongdongnan Basin. Acta Petrolei Sinica (in Chinese), 31(4): 542–547
Li Youchuan, Mi Lijun, Zhang Gongcheng, et al. 2011. The formation and distribution of source rocks for deep water area in the Northern of South China Sea. Acta Sedimentologica Sinica (in Chinese), 29(5): 970–979
Li Shuxia, Shao Longyi, Liu Jinshui, et al. 2022. Oil generation model of the liptinite-rich coals: Palaeogene in the Xihu Sag, East China Sea Shelf Basin. Journal of Petroleum Science and Engineering, 209: 109844, doi: 10.1016/j.petrol.2021.109844
Li Xianqing, Zhong Ning, Ning Xiongbo, et al. 1997. A study on thermal evolution of organic matter in coal-bearing source rocks of Xihu Sag. Coal Geology of China (in Chinese), 9(1): 33–36
Liu Guangdi. 2009. Petroleum geology (in Chinese). 4th ed. Beijing: Petroleum Industry Press, 160
Liu Zhifeng, Wu Keqiang, Ke Ling, et al. 2017. Main factors controlling hydrocarbon accumulation in northern subsag belt of the Zhu-1 Depression, Pearl River Mouth Basin. Oil & Gas Geology (in Chinese), 38(3): 561–569
Liu Gang, Zhou Dongsheng. 2007. Application of microelements analysis in identifying sedimentary environment-taking Qianjiang formation in the Jianghan Basin as an example Petroleum Geology and Experiment. Petroleum Geology & Experiment (in Chinese), 29(3): 307–310,314
Lu Jing, Shao Longyi, Yang Minfang, et al. 2014. Coal facies evolution, sequence stratigraphy and palaeoenvironment of swamp in terrestrial basin. Journal of China Coal Society (in Chinese), 39(12): 2473–2481
Ma Zuochun, Chen Daoxiu, Zhang Jinglong, et al. 1989. Oil-Source Correlation and Coal-Derived Oil Discussion. See the Third Collection of Petroleum Geology Research Reports in the Eastern Pearl River Mouth Basin, Edited by the Institute of Exploration and Development of the Eastern South China Sea Petroleum Company. (in Chinese). Kwangchow: Institute of Eastern South China Sea Petroleum Company, 9–12
Mao Wanhui, Zhuang Xinguo, Zhou Jibing, et al. 2011. Application of coal facies parameters in sequence stratigraphic division of coal seams: with Zhangnanxi coal district, Junggar basin as example. Coal Geology & Exploration (in Chinese), 39(1): 6–10
Pang Xiong, Shi Hesheng, Zhu Ming, et al. 2014. A further discussion on the hydrocarbon exploration potential in Baiyun deep water area. China Offshore Oil and Gas (in Chinese), 26(3): 23–29
Pepper A S, Corvi P J. 1995. Simple kinetic models of petroleum formation. Part Ⅲ: Modelling an open system. Marine & Petroleum Geology, 12(4): 417–452
Peters K E, Cassa M R. 1994. Applied source rock geochemistry. In: Magoon L B, Dow W G, eds. The Petroleum System-from Source to Trap. AAPG Memoir, 60: 93–120
Peters K E , Moldowan J M. 1993. The Biomarker Guide: Interpreting Molecular Fossils in Petroleum and Ancient Sediments. Englewood Cliffs Nj Prentice Hall
Shen Wenchao. 2018. The coal accumulation model and sedimentary organic facies of Paleogene coal in the Xihu Depression (in Chinese)[dissertation]. Beijing: China University of Mining and Technology
Shen Yulin, Qin Yong, Guo Yinghai, et al. 2016. Development characteristics of coal-measure source rocks divided on the basis of Milankovich coal accumulation cycle in Pinghu Formation, Xihu sag. Acta Petrolei Sinica (in Chinese), 37(6): 706–714
Shu Yu, Shi Hesheng, Du Jiayuan, et al. 2014. Paleogene characteristics in hydrocarbon accumulation and exploration direction in Zhu Ⅰ depression. China Offshore Oil and Gas (in Chinese), 26(3): 37–42
Suárez-Ruiz I, Crelling J C. 2008. Applied Coal Petrology. Amsterdam: Elsevier, 19–60
Sykes R, Snowdon L R. 2002. Guidelines for assessing the petroleum potential of coaly source rocks using Rock-Eval pyrolysis. Organic Geochemistry, 33(12): 1441–1455, doi: 10.1016/S0146-6380(02)00183-3
Thompson, Cooper B S, Morley R J, et al. , 1985. Oil-generating coal, In: Thomas, B. M (eds), Petroleum geochemistry of the Norwegian shelf, London: Graham and Trotman

Tang Yuegang, Guo Xin, Li Zhengyue, et al. 2020. Characteristics and coal facies of high quality anthracite from coal seam No. 5 of Xiaofalu coal mine, Yunnan province. Journal of Mining Science and Technology (in Chinese), 5(1): 12–21

Tissot B P, Welte D H. 1984. Coal and its relation to oil and gas. In: Petroleum Formation and

Vandenbroucke M, Largeau C. 2007. Kerogen origin, evolution and structure. Organic Geochemistry, 38(5): 719–833, doi: 10.1016/j.orggeochem.2007.01.001

Wang Dongdong, Dong Guoqi, Zhang Gongcheng, et al. 2020. Coal seam development characteristics and distribution predictions in marginal sea basins: Oligocene Yacheng Formation coal measures, Qiongdongnan Basin, northern region of the South China Sea. Australian Journal of Earth Sciences, 67(3): 393–409, doi: 10.1080/08120099.2019.1661286

Wang Zhenfeng, Li Xushen, Sun Zhipeng, et al. 2011. Hydrocarbon accumulation conditions and exploration potential in the deepwater region, Qiongdongnan Basin. China Offshore Oil and Gas (in Chinese), 23(1): 7–13,31

Wang Shaoqing, Tang Yuegang. 2007. Coal petrological characteristics and coal facies in Shendong mining area. Coal Geology of China (in Chinese), 19(5): 4–7,15

Wang Liangchen, Zhang Jinliang. 1996. Sedimentary environment and sedimentary facies (in Chinese). Being: Petroleum Industry Press, 146–147

Wei Xiaosong, Yan Detian, Luo Pan, et al. 2020. Astronomically forced climate cooling across the Eocene–Oligocene transition in the Pearl River Mouth Basin, northern South China Sea. Palaeogeography, Palaeoclimatology, Palaeoecology, 558: 109945

Wilkins R W T, George S C. 2002. Coal as a source rock for oil: a review. International Journal of Coal Geology, 50(1–4): 317–361, doi: 10.1016/S0166-5162(02)00134-9

Wu Juan. 2013. Enrichment regularity of Zhu I Depression, Peal River Mouth Basin (in Chinese)[dissertation]. Wuhan: China University of Geosciences

Xie Xinong, Zhang Cheng, Ren Jianye, et al. 2011. Effects of distinct tectonic evolutions on hydrocarbon accumulation in northern and southern continental marginal basins of South China Sea. Chinese Journal of Geophysics (in Chinese), 54(12): 3280–3291

Xie Ruiyong, Zhao Fei. 2015. Discussion on sedimentary organic facies of source rocks in Baiyun Sag, Pearl River Mouth Basin. Energy Technology and Management (in Chinese), 40(6): 7–9.

Yang Jianye, Ren Deyi, Shao Longyi. 2000. The distribution of sedimentary organic facies in the continental facies sequence stratigraphic framework: an example from Middle Jurassic coal-bearing series in the Taibei sag of the Turpan-Hami basin and Southern Junggar basin. Acta Sedimentologica Sinica (in Chinese), 18(4): 585–589

Yang Chupeng, Yao Yongjian, Li Xuejie, et al. 2010. Oil-generating potential of Cenozoic coal-measure source rocks in Zengmu Baisn, the southern South China Sea. Acta Petrolei Sinica (in Chinese), 31(6): 920–926

Yao Yifeng. 2006. Eocene palynoflora form Changchang Basin, Hainan Island and its bearing on the implications of palaeovegetation and palaeoclimate (in Chinese)[dissertation]. Beijing: The Institute of Botany, Chinese Academy of Sciences

Yao Yongjian, Wu Nengyou, Xia Bin, et al. 2008. Petroleum geology of the Zengmu basin in the southern South China Sea. Geology in China (in Chinese), 35(3): 503–513

Zhang Juan. 2017. Maturity determination of hydrocarbon source rocks in Xihu Sag: evidence from fluorescence alteration of multiple macerals. Petroleum Geology & Experiment (in Chinese), 39(3): 417–422

Zhang Gongcheng, Chen Ying, Li Zengxue, et al. 2022. Theory on genesis of coaliferous petroleum in the China Sea. Oil & Gas Geology (in Chinese), 43(3): 553–565

Zhang Gongcheng, Chen Ying, Wang Dongdong, et al. 2023. Cenozoic giant coal-bearing basin belt discovered in China's sea area. Acta Oceanologica Sinica, 42(3): 101–112, doi: 10.1007/s13131-022-2134-x

Zhang Gongcheng, Li Zengxue, He Yuping, et al. 2010. Coal geochemistry of Qiongdongnan Basin. Natural Gas Geoscience (in Chinese), 21(5): 693–699

Zhang Gongcheng, Li Youchuan, Xie Xiaojun, et al. 2016a. Tectonic cycle of marginal sea controls the ordered distribution of source rocks of deep water areas in South China Sea. China Offshore Oil and Gas (in Chinese), 28(2): 23–36

Zhang Gongcheng, Mi Lijun, Wu Shiguo, et al. 2007. Deepwater area-the new prospecting targets of northern continental margin of South China Sea. Acta Petrolei Sinica (in Chinese), 28(2): 15–21

Zhang Gongcheng, Qu Hongjun, Zhao Chong, et al. 2017a. Giant discoveries of oil and gas exploration in global deepwaters in 40 years and the prospect of exploration. Natural Gas Geoscience (in Chinese), 28(10): 1447–1477

Zhang Chunliang, Shen Yulin, Qin Yong, et al. 2016b. Development regularities of the coal-measure source rock in Ya-3 member of Yacheng Formation, Well Y1, in Yanan Depression within Qiongdongnan Basin. Acta Sedimentologica Sinica (in Chinese), 34(5): 1003–1010

Zhang Lili, Shu Liangfeng, Feng Xuan, et al. 2020. Further discussion on the age assignment of Enping Formation in the Pearl River Mouth Basin. China Offshore Oil and Gas (in Chinese), 32(5): 9–18

Zhang Gongcheng, Tang Wu, Xie Xiaojun, et al. 2017b. Petroleum geological characteristics of two basin belts in southern continental margin in South China Sea. Petroleum Exploration and Development (in Chinese), 44(6): 849–859

Zhang Gongcheng, Wang Dongdong, Zeng Qingbo, et al. 2019. Characteristics of coal-measure source rock and gas accumulation belts in marine-continental transitional facies fault basins: A case study of the Oligocene deposits in the Qiongdongnan Basin located in the northern region of the South China Sea. Energy Exploration & Exploitation, 37(6): 1752–1778

Zheng Rongcai, Liu Meiqing. 1999. Study on palaeosalinity of Chang 6 Oil Reservoir set in Ordos Basin. Oil & Gas Geology (in Chinese), 20(1): 20–25

Zhu Xiaomin, Huang Handong, Dai Yiding, et al. 2014. Study on depositional system and sequence framework of Wenchang Formation in Panyu 4 depression of the Pearl River Mouth Basin. Lithologic Reservoirs (in Chinese), 26(4): 1–8